# Biomagnetism:

## Detection and Imaging Weak Magnetic Fields from the Human Body

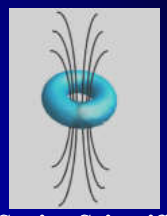

Senior Scientific

The University of New Mexico

# Senior Scientific, LLC:

A private business with NIH SBIR funding.

Primary Mission: Disease detection using magnetic nanotechnology.

PI: Edward R. Flynn, PhD Physicist

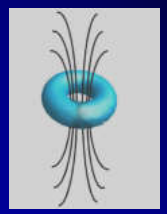

Senior Scientific

The University of New Mexico

# Outline of Talk

## Detection and Imaging of Weak Biomagnetic Fields

1) SQUID Sensors
2) Experimental Apparatus
3) Imaging the Brain
4) Imaging the Mind
5) Detection and Imaging Disease

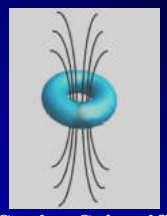

Senior Scientific

The University of New Mexico

# Magnetic Field Strengths of various sources and Sensor Sensitivities

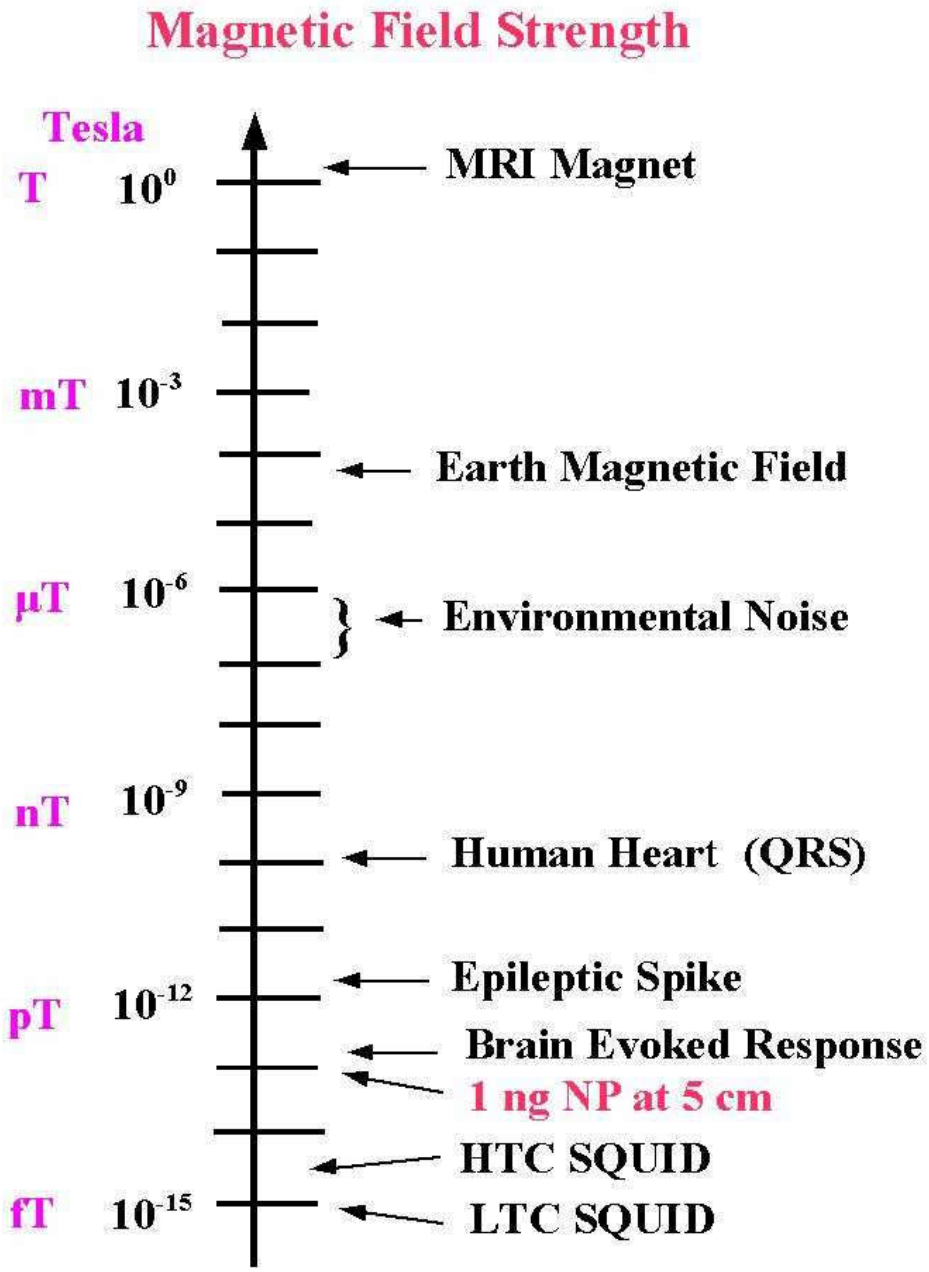


Senior Scientific

The University of New Mexico

# MEG
## Magnetoencephalography

Measurement of the natural magnetic fields
From the brain arising from neuronal currents

A: Instrumentation

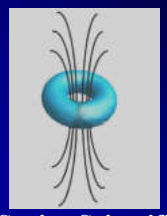

Senior Scientific

The University of New Mexico

# What is a SQUID?

Superconducting Quantum Interference Device (SQUID)

Quantum Mechanical (Josephson) Tunneling in a Superconductor

Sensor must have no resistive noise so superconducting material is used.

- LTC SQUIDs are sensitive down to ~ 3 fT

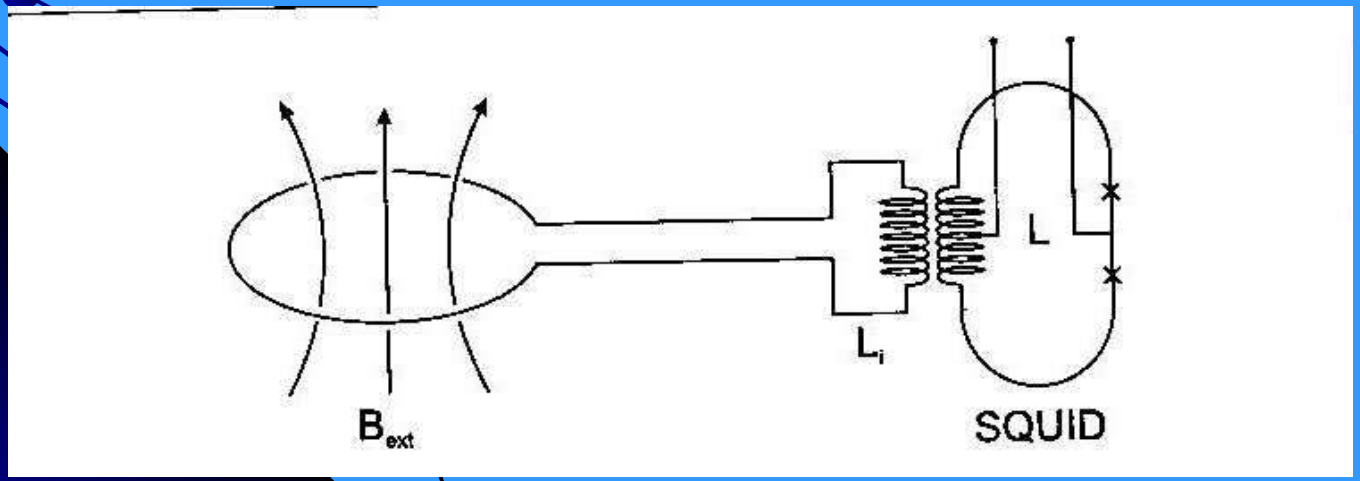


Senior Scientific

The University of New Mexico

# Basics of SQUID Operation

$$I = I_c \sin\theta \ ,$$

$$\frac{\partial\theta}{\partial t} = 2\pi V \frac{2e}{h} = \frac{2\pi V}{\Phi_0}$$

Josephson Equations: Θ is phase across junction, I=current, V= junction voltage, $\Phi_a$ = h/2e=2.07 fWb (flux quanta)

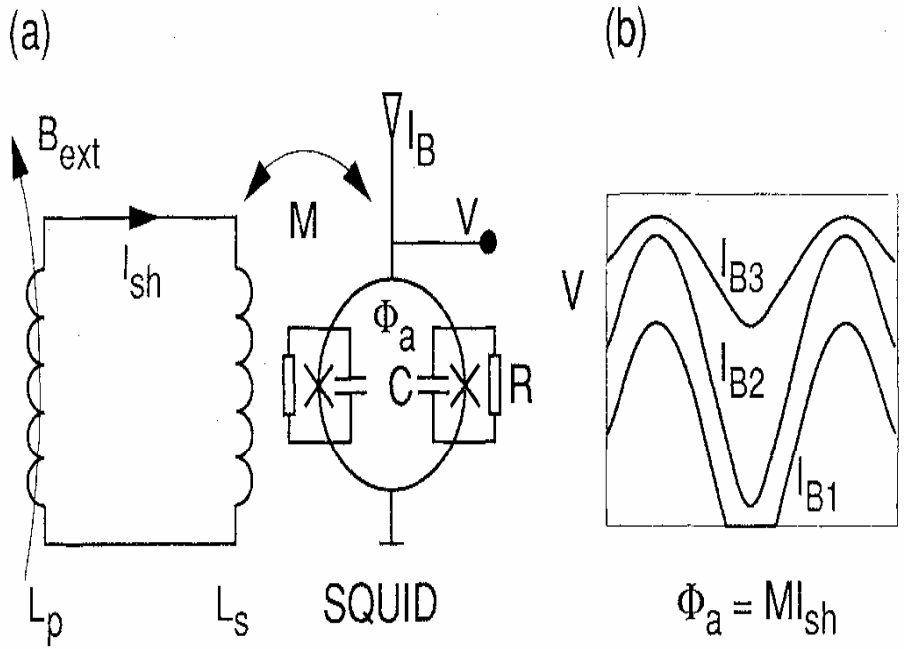


(a) Schematic diagram of DC SQUID, $L_s$ is superconducting flux transformer

(b) Voltage across SQUID depends on bias I, and is periodic function of the incident flux $\Phi_a$ .

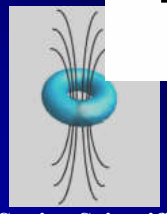

Senior Scientific

The University of New Mexico

# Principles of MEG

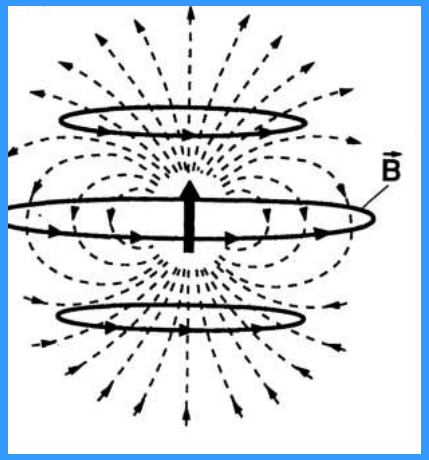


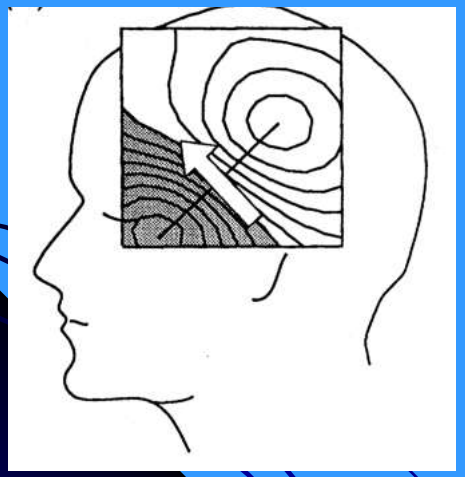

Current Dipole

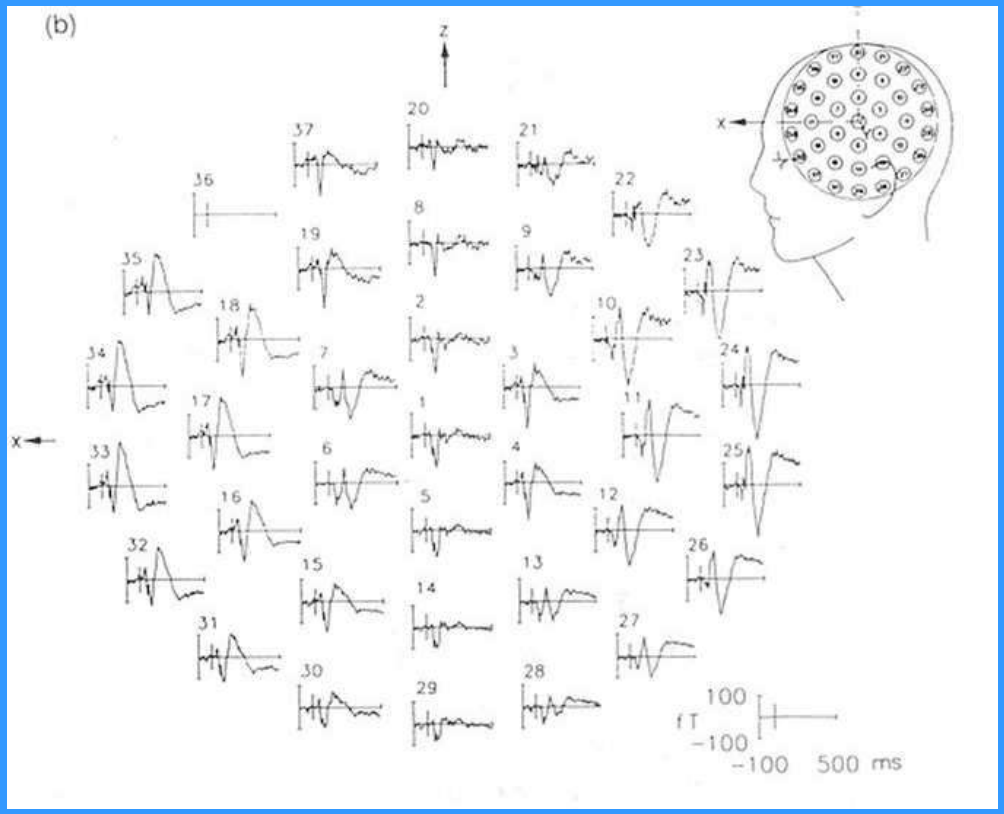


Field amplitude vs time for a sensor array – Evoked Response

Magnetoencephalography—theory, instrumentation, and applications to noninvasive studies of the working human brain

Matti Hämäläinen, Riitta Hari, Risto J. Ilmoniemi, Jukka Knuutila, and Olli V. Lounasmaa

Reviews of Modern Physics, Vol. 65, No. 2, April 1993

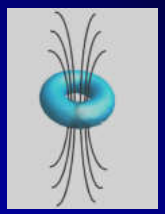

Senior Scientific

The University of New Mexico

# The SISG MEG System

Superconducting "helmet" made of a thin lead sheet.

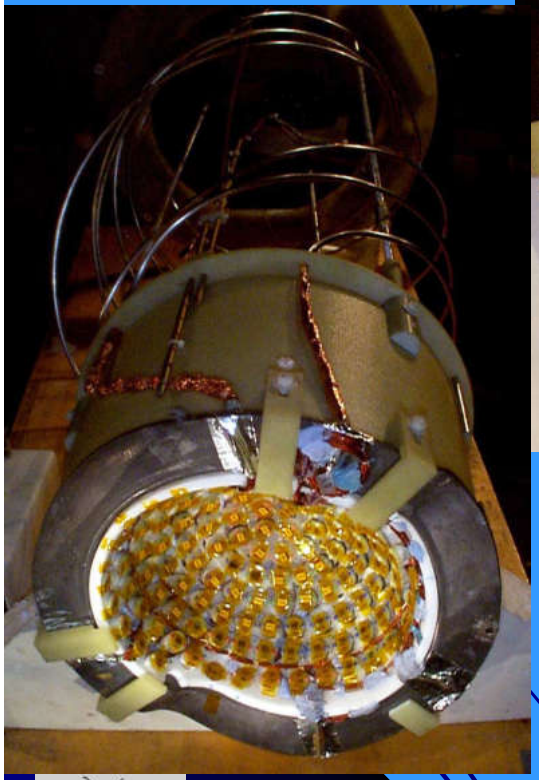

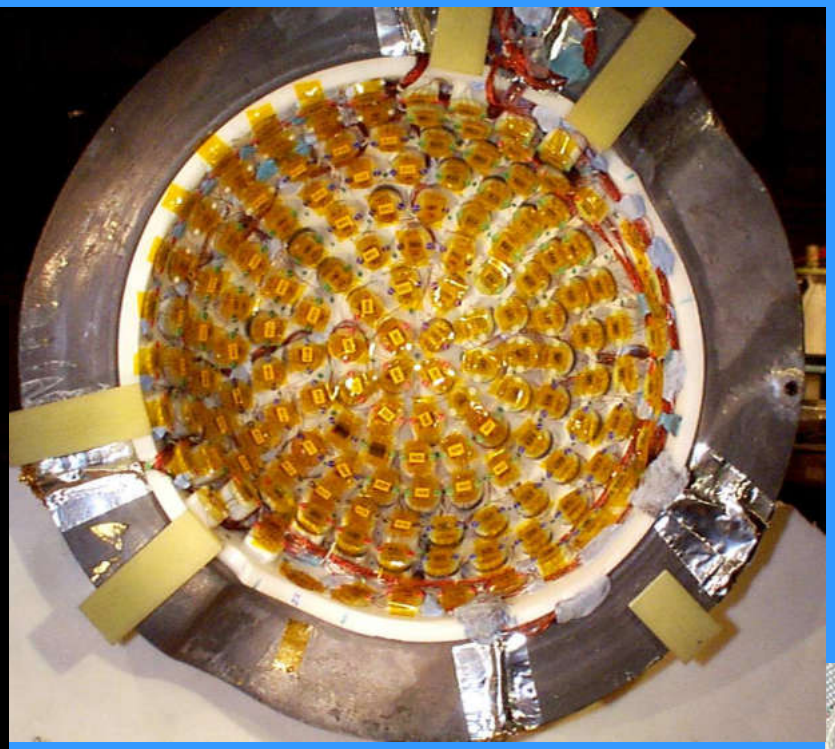

155 ch SQUID array installed inside superconducting imaging surface "helmet"

Integrated SQUID sensors and pickup coils

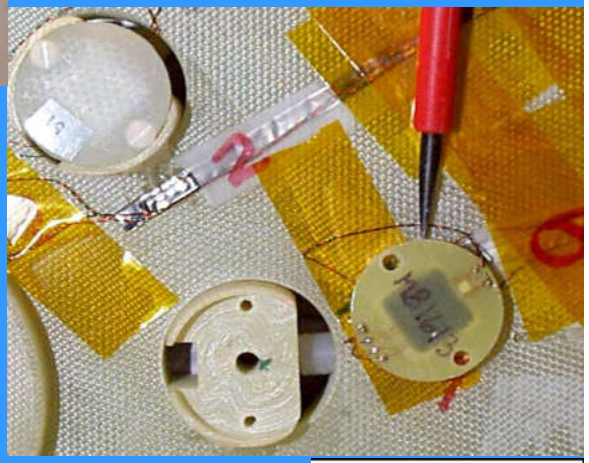

A large array sensor for MEG based on the superconducting imaging surface gradiometer concept.

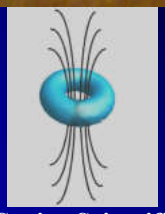

Senior Scientific

The University of New Mexico

The Dewar

Liquid helium

- 248 axial gradiometers (low noise)
- 1 kHz sampling rate

The MEG instrument at the Minneapolis Domenici Center
(Magnes 3600WH, 4-D Neuroimaging, San Diego, CA)

Senior Scientific

The University of New Mexico

# MEG
## Magnetoencephalography

Imaging the Brain

SpatioTemporal Analysis of Sensor Magnetic Fields to Image Brain Sources using EM Inverse Solutions

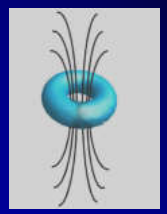

Senior Scientific

The University of New Mexico

# SQUIDs Measure Both Space and Time

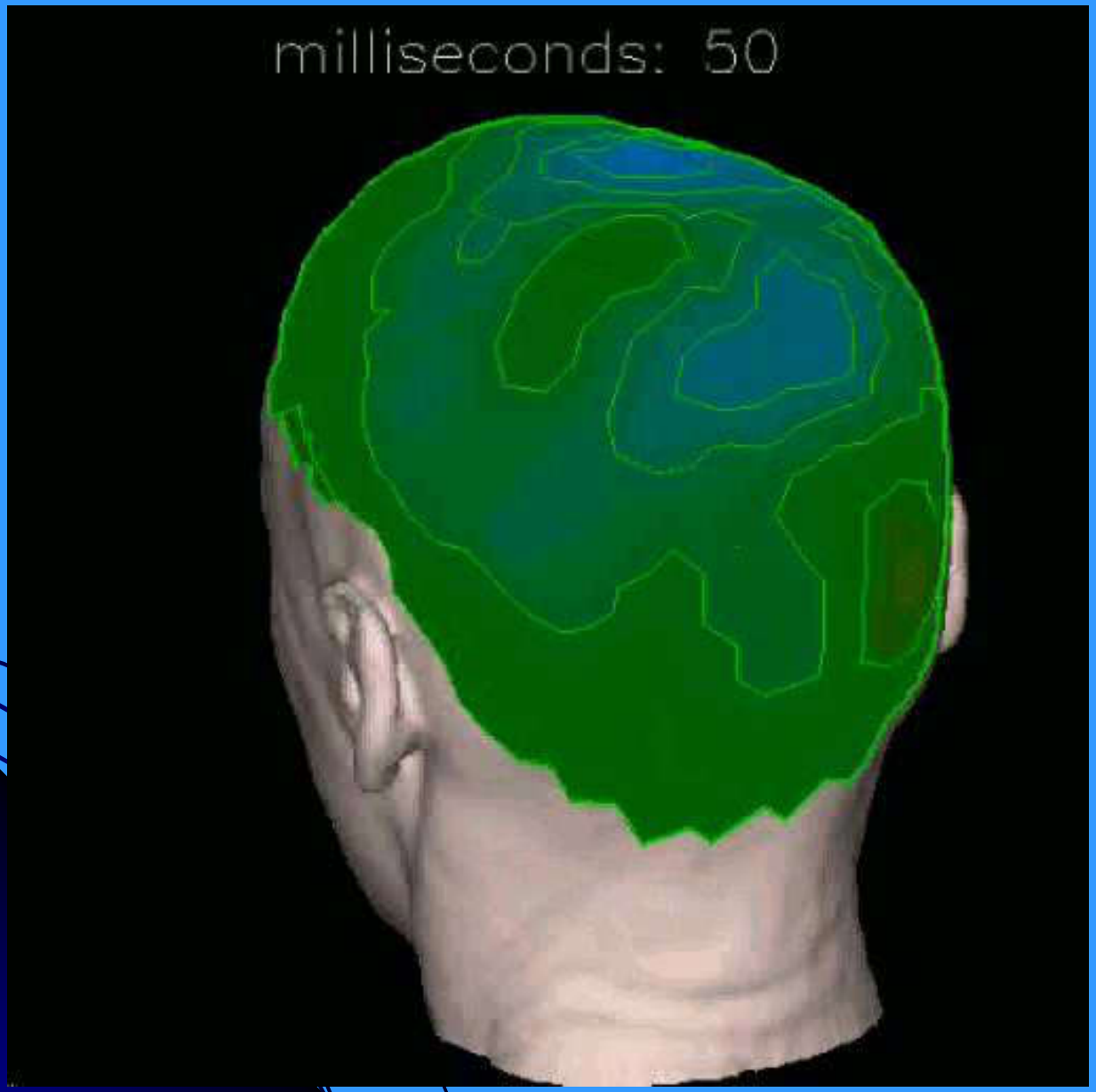


Magnetic field contour lines, plotted here as a function of time, are used to determine neural sources.

Response of the brain to a visual stimulus.

Senior Scientific

The University of New Mexico

# Finding the Sources with a Spatial-Temporal algorithm

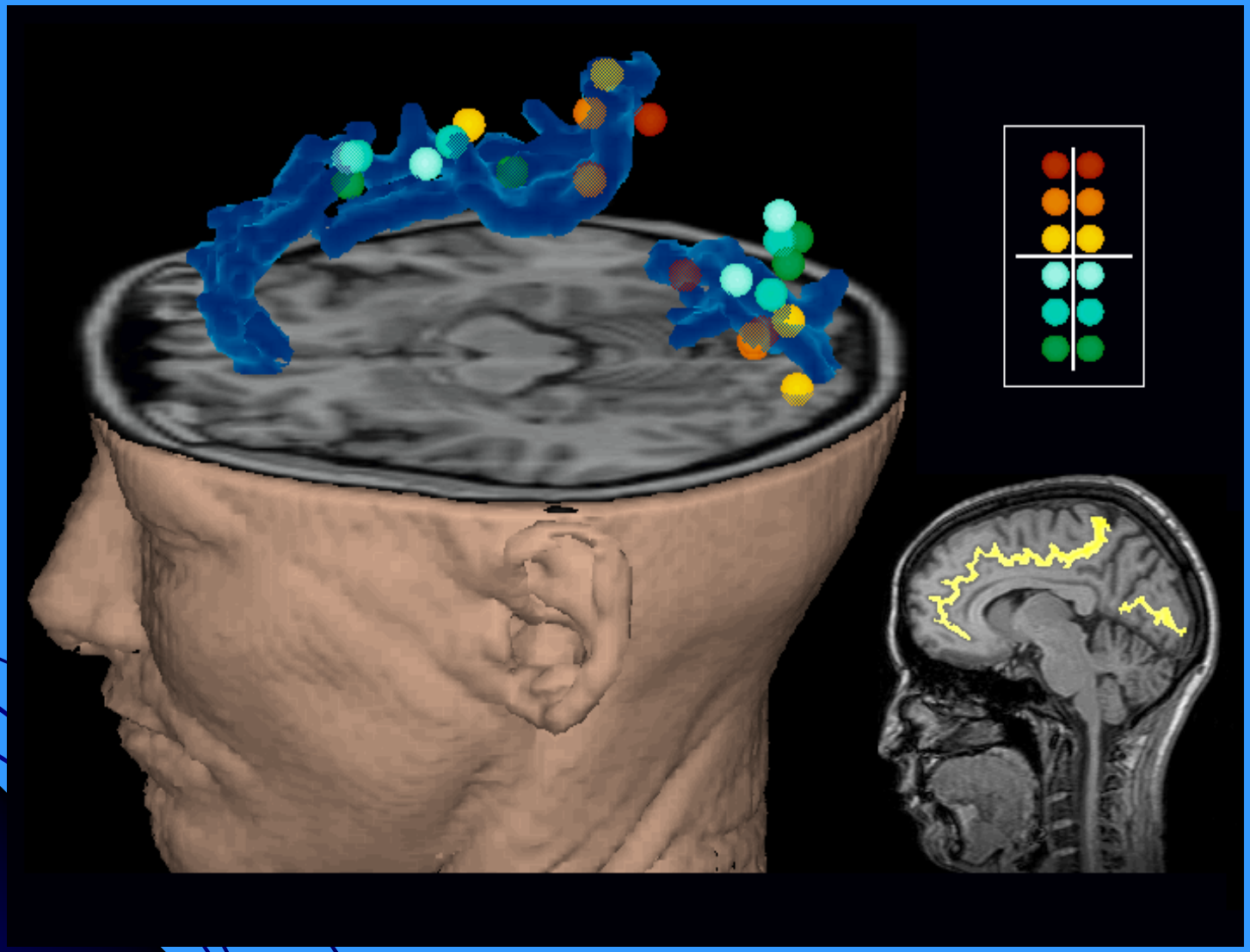

Graphics by
Ranken LANL

Senior Scientific

The University of New Mexico

# MEG
## Magnetoencephalography

Imaging the Mind

Examine correlations between magnetic field magnitude and time in sensor space

(No inverse problem)

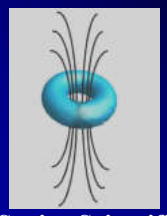

Senior Scientific

The University of New Mexico

# Data Analysis - 1

Analyses are performed to estimate quantitatively the synchronous (i.e. zero-lag) interactions between signals from pairs of sensors to assess dynamic brain function.

- **Step 1**: Calculate all pairwise zero-lag cross-correlations
- **Step 2**: Calculate the partial zero-lag cross-correlations within the 248-sensor network

Langheim, F.J.P., Leuthold, A.C. and Georgopoulos, A.P. (2006) Synchronous dynamic brain networks revealed by magnetoencephalography (MEG) Proceedings of the National Academy of Sciences USA 103: 455-459.

# Data Analysis - 2

- The MEG time series are "**prewhitened**" by fitting an ARIMA (AutoRegressive Integrative Moving Average) Box-Jenkins model and taking the residuals

- This procedure yields practically stationary series from which CCF is estimated

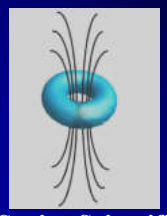

Senior Scientific

The University of New Mexico

# Zero-lag (1-ms synchronous) Partial Correlations Of Prewhitened (stationary) MEG Time Series

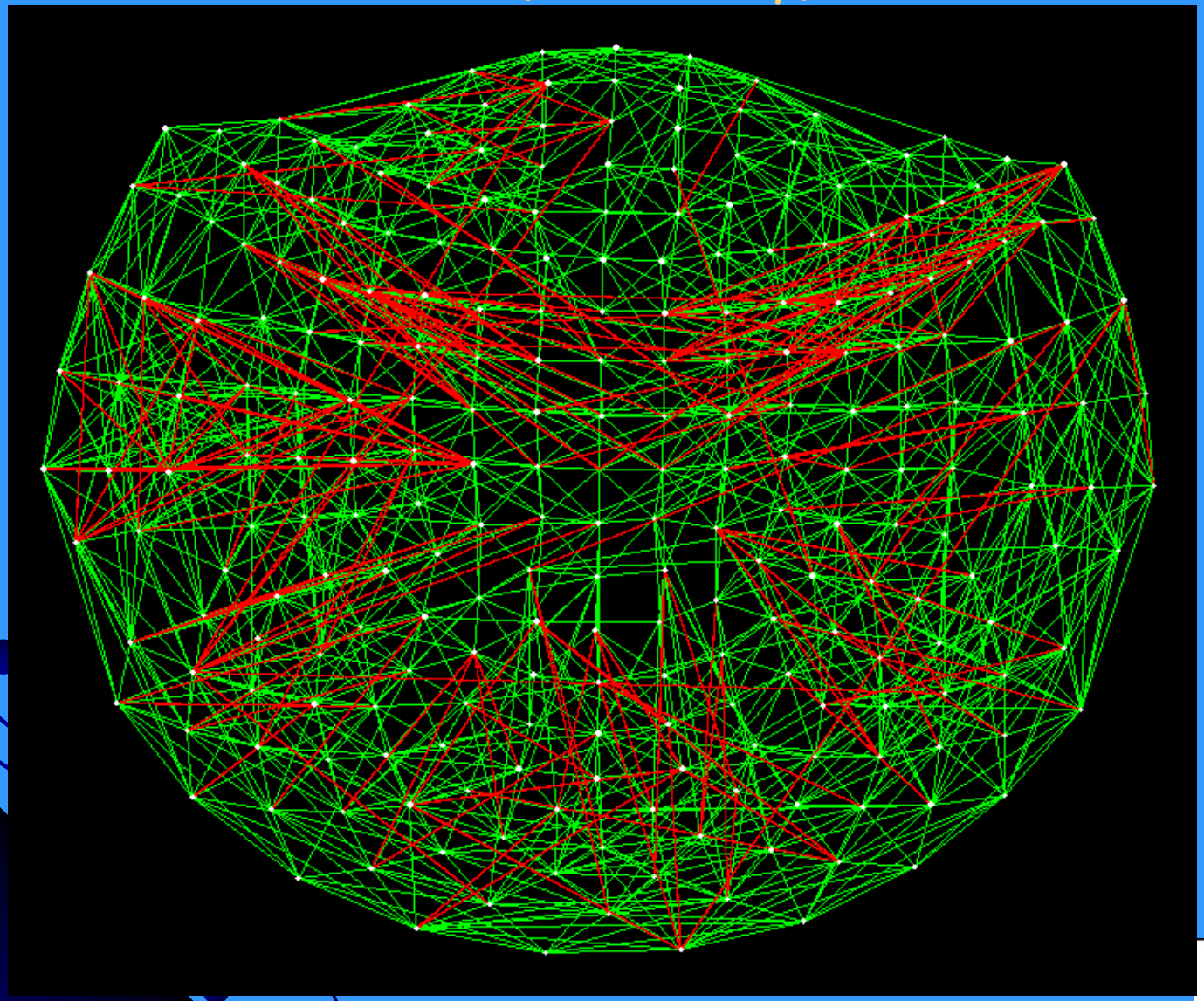

Langheim et al., PNAS, 2006

Senior Scientific

The University of New Mexico

# Predictions from raw MEG signals: Music Perception

- Subjects listened to a musical piece while MEG was recorded
- Single trials analyzed using multivariate regression of MEG data on MIDI notes of the piece
- Predicting MIDI notes listened to

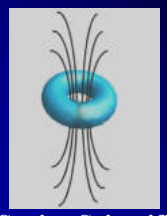

Senior Scientific

The University of New Mexico

# Music Stimulus A

PPanther_Stimulus

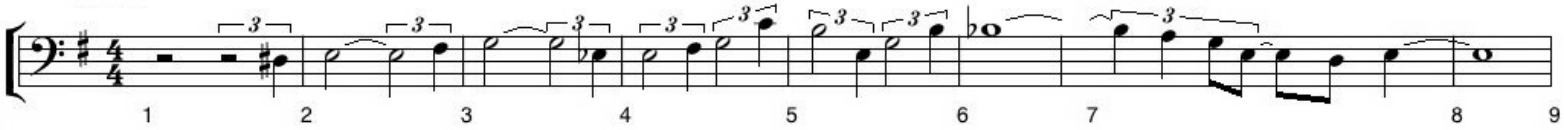


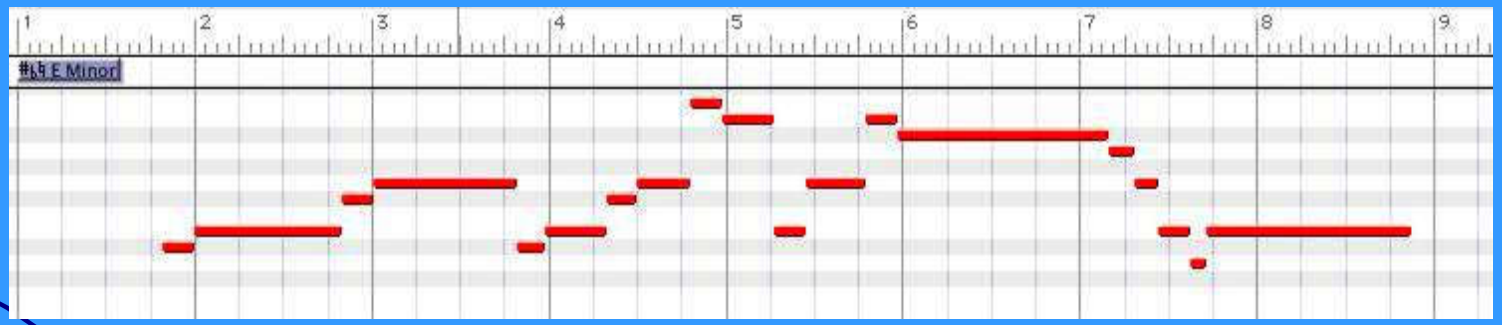

# Music Prediction A

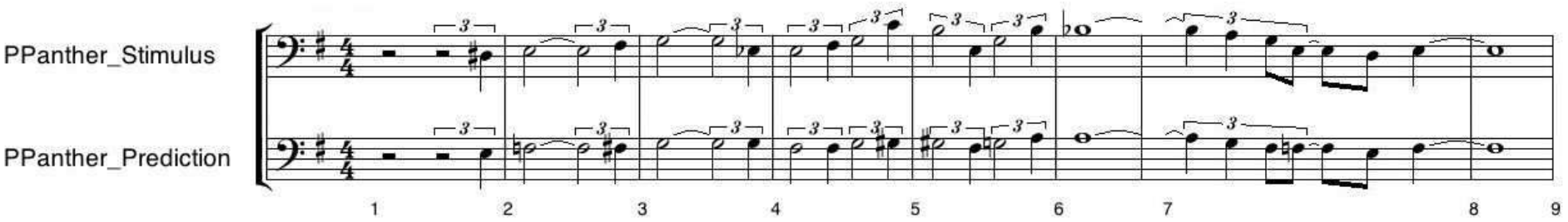


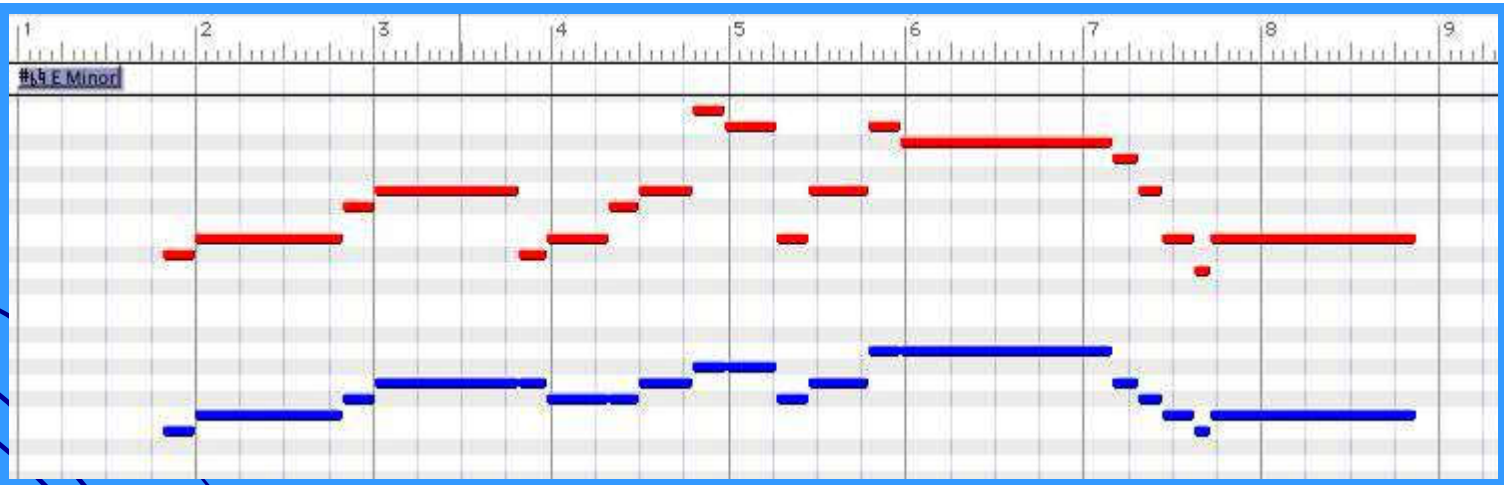

# Assessment of Dynamic Brain Function: Synchronous Neural Networks

- Examine correlations between magnetic field magnitude and time in sensor space
- All possible zero-lag partial cross-correlations between 248 sensors (= 30,628)
- Positive or negative
- 1-ms temporal resolution = true synchronicity
- Simple fixation – look at a dot for 45 – 60 sec

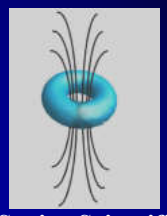

Senior Scientific

The University of New Mexico

# Discriminant classification analysis

- Linear discriminant analysis
- Robust, cross-validated leave-one-out method
- 100% correct classification of 52 subjects to one of 6 groups (healthy control, Alzheimer's Disease, schizophrenia, chronic alcoholic, multiple sclerosis, Sjögren's syndrome) using as few as 10 zero-lag cross-correlations as predictors!
- Such sets are found in numbers far in excess of those expected by chance

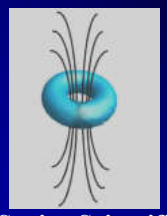

Senior Scientific

The University of New Mexico

# Canonical Discriminant Functions

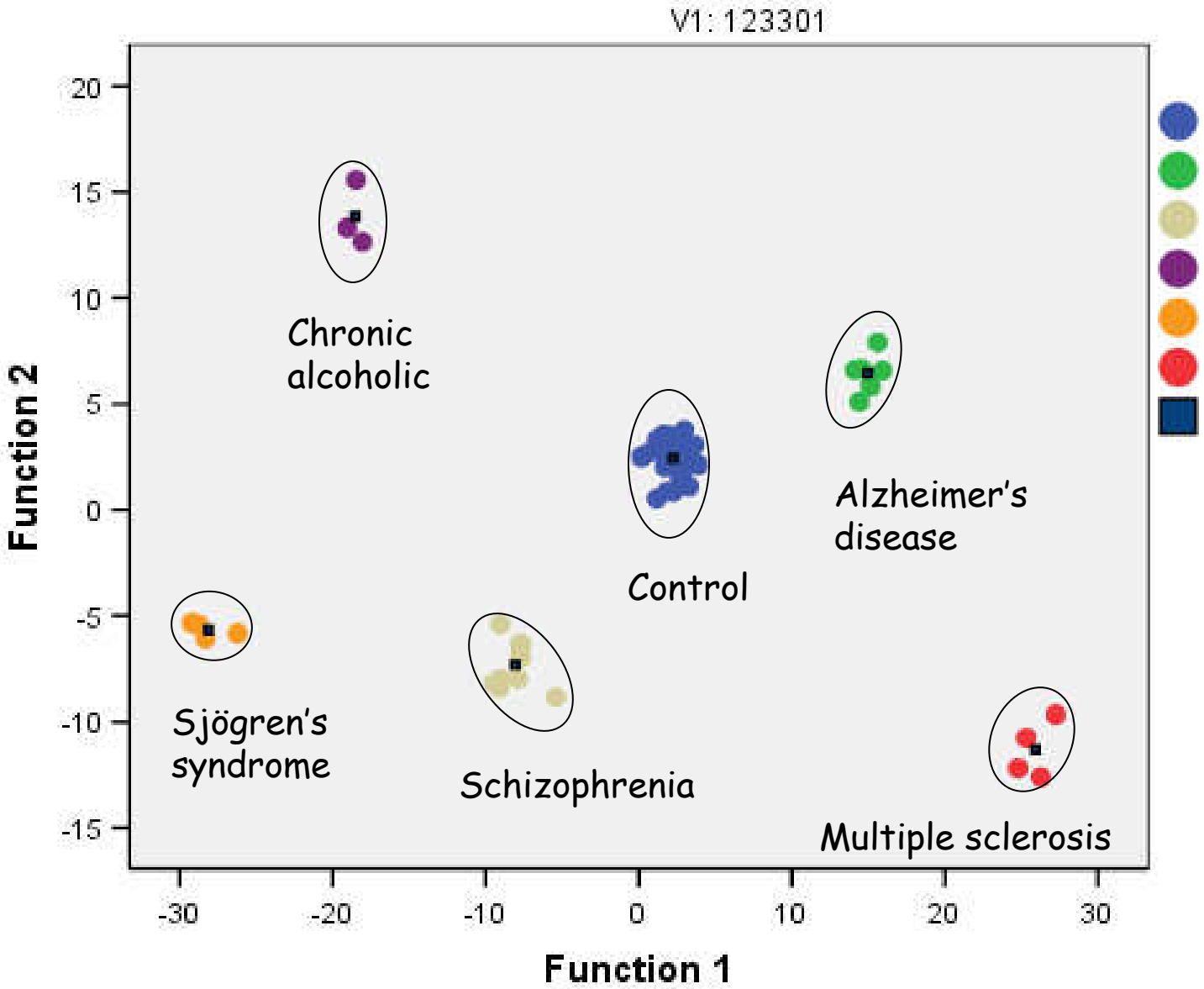


40 predictors

Senior Scientific

The University of New Mexico

# Superparamagnetic Particles and the Detection and Imaging of Disease using Magnetic Sensors

## Superparamagnetism

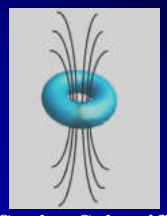

Senior Scientific

The University of New Mexico

# Magnetic Nanoparticle with antibody attached

Typical magnetic core diameter is 20 –30 nm.

Typical bio-coatings are: Carboxyl, starch, streptavidin, PEG

Antibodies are specific markers for various types of cells; e.g., T-cells, various types of cancer cells, etc.

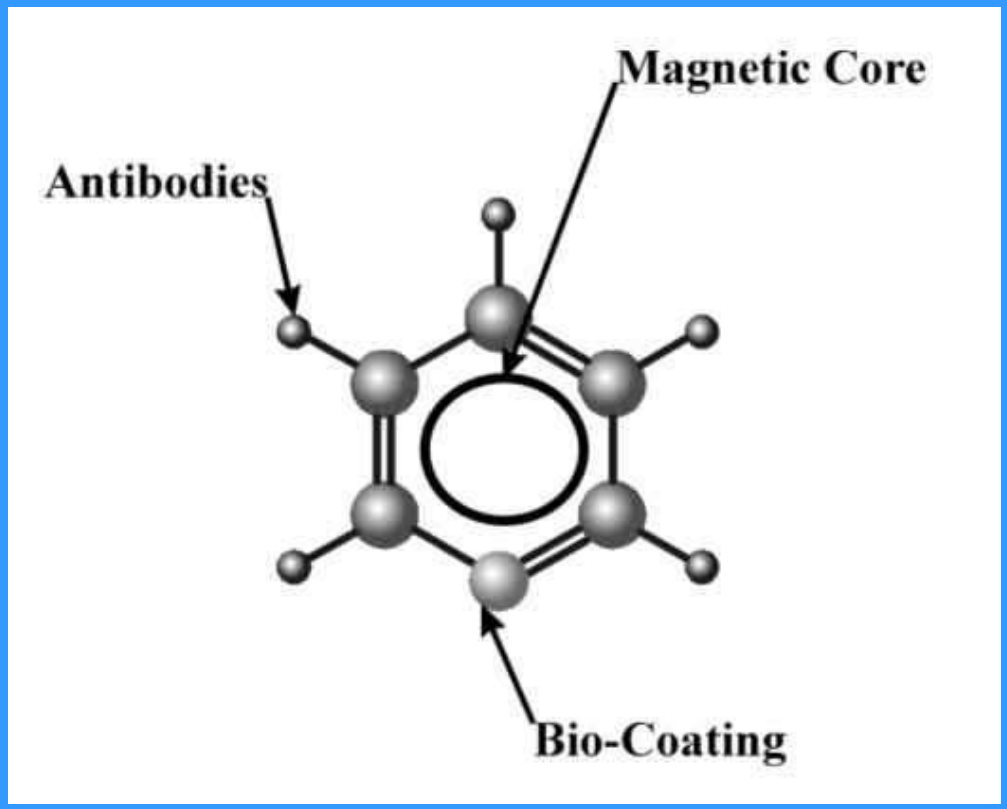


Senior Scientific

The University of New Mexico

# Superparamagnetism

Iron-oxide nanoparticles <100 nm diameter

Particles consist of a single magnetic domain.

All internal atomic magnetic moments are aligned (homogeneous magnetization)

Free particles randomize quickly by Brownian Motion

Bound particles decay by Néel Mechanism

Particles exhibit large magnetic moments when magnetized

Particles behave as paramagnetic when not magnetized (they do not agglomerate)

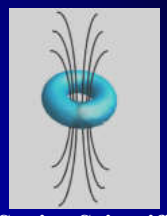

Senior Scientific

The University of New Mexico

# Scanning Electron Microscope View of Nanoparticles

Monodisperse magnetite 20 nm diameter, made at Center for Integrative Nanotechnology at Sandia National Laboratory (Dale Huber)

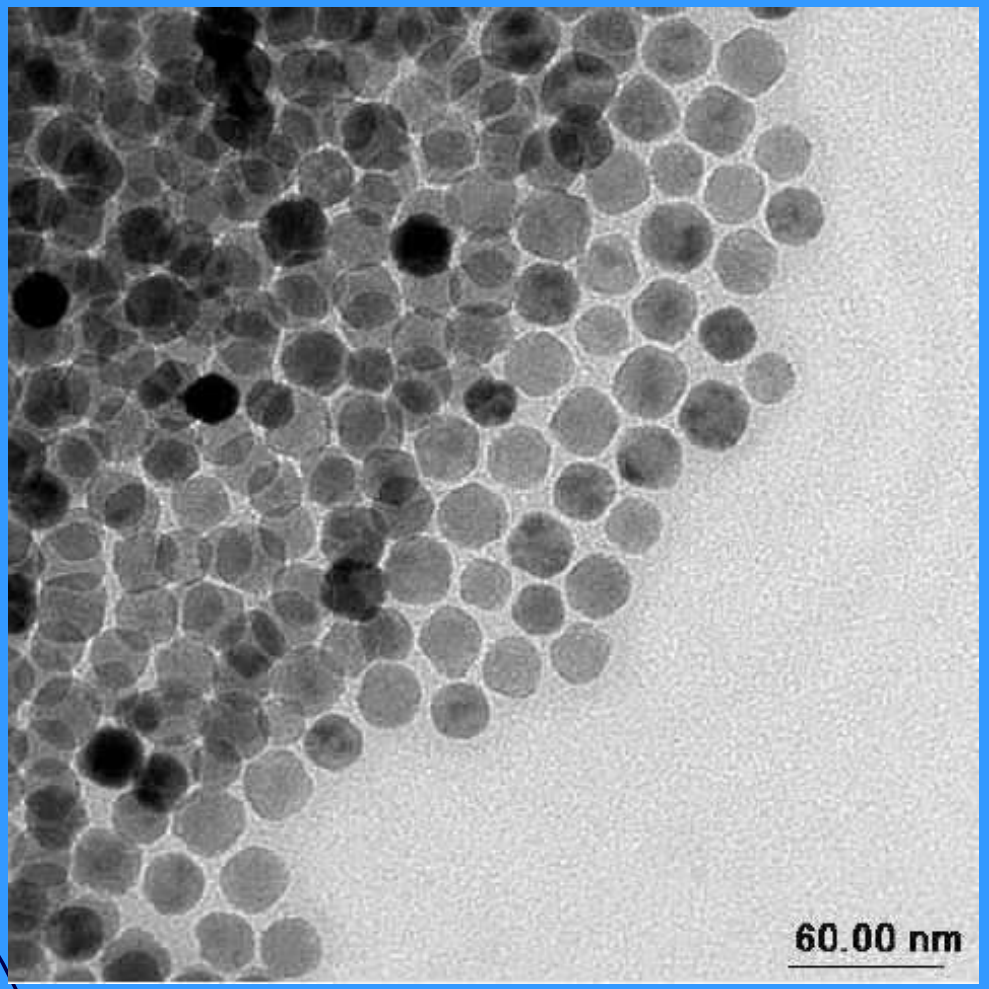


Senior Scientific

The University of New Mexico

# Nanoparticles form a Magnetic Dipole when a magnetizing pulse is applied

- An induced collective dipole moment μ(t) is the result of alignment of a collection of N particles each with a moment $\mu_p$ by an external pulsed field B for a duration $t_0$.

- μ(t) decays as the individual particle orientations relax, this is called the remanence time.

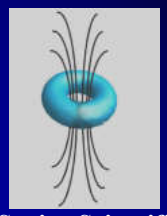

Senior Scientific

The University of New Mexico

# The interaction of a nanoparticle of magnetic moment $\mu$ with a magnetic field

$$U = -\vec{\mu} \cdot \vec{B}$$

The average value of the cosine of the angle between is

$$\overline{\cos\theta} = \int e^{-U/kT} \cos\theta d\Omega / \int e^{-U/kT} d\Omega$$

The Langevin function, L(x) gives the average value of cos θ where x= μB/kT

$$L(x) = \coth(x) - 1/x$$

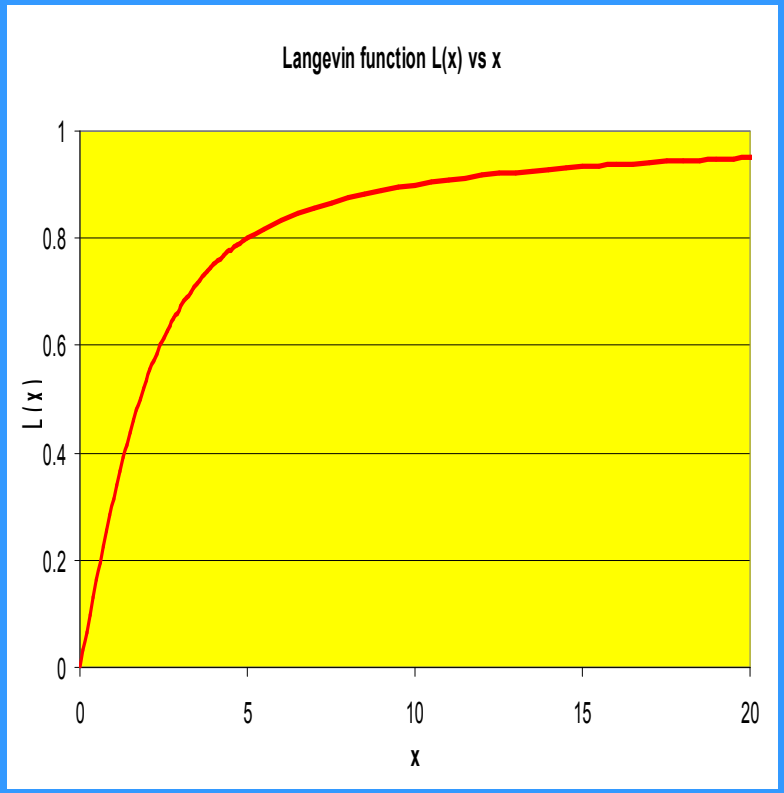


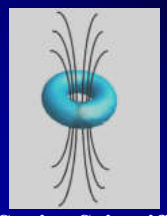

Senior Scientific

The University of New Mexico

# Dipole formed by the magnetic pulse and its decay

Each nanoparticle of radius r is aligned by the field of pulsed Helmholtz coils to form an initial moment determined by the Langevin function and the Néel relaxation time:

$$\mu_0(r,t_0,B) = \mu_p L(x)[1-\exp(t_0/\tau(r,B))]$$

The decaying dipole seen by a SQUID is the sum of all the aligned nanoparticle moments as they randomize when the field is quenched.

$$\mu(t,t_0,B) = N\int_0^\infty drP(r)\mu_0(r,t_0,B)\exp(-t/\tau(r,0))$$

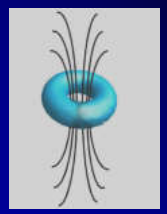

Senior Scientific

The University of New Mexico

# Brownian vs Néel Relaxation Times

## Free Particles

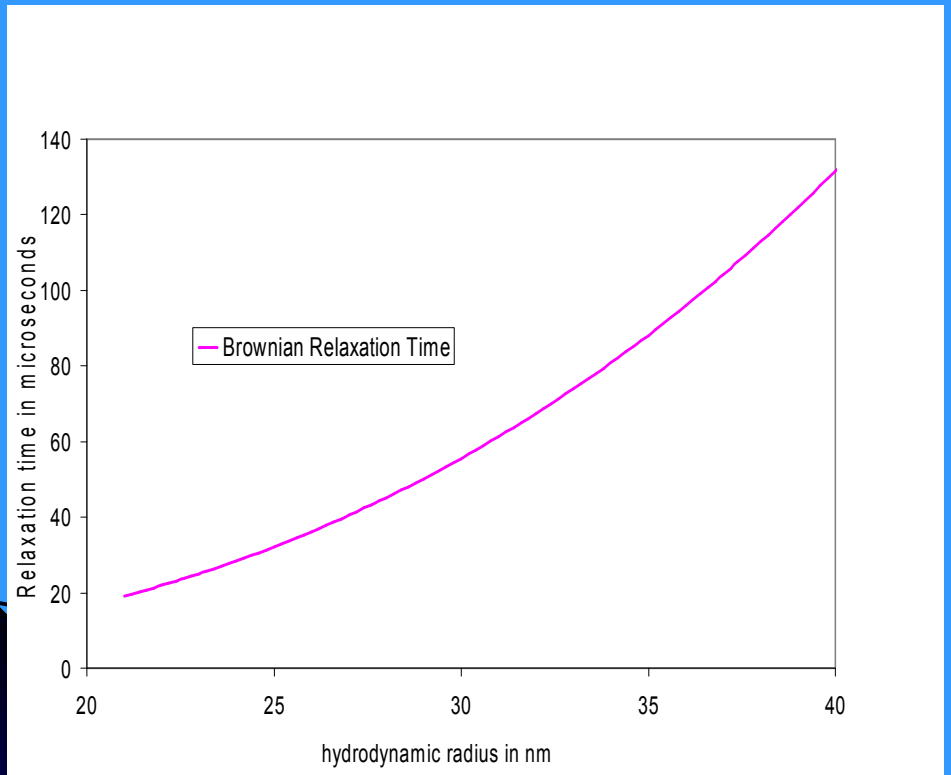


## Bound Particles

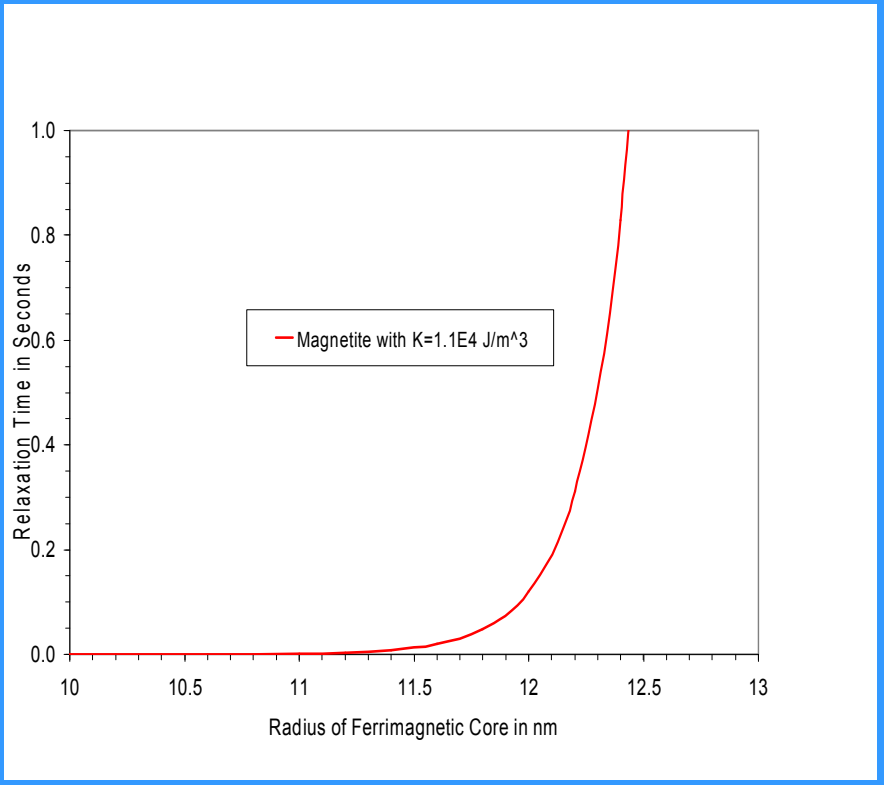


## Brownian

$$\tau_{Brownian} = 4\pi\eta R^3 / kT$$

## Néel

$$\tau_{Neel} = \tau_0 \exp(KV / kT)$$

For polydisperse nanoparticles

$B(t) = a_0 + a_1 * \ln(1+b/t)$

Senior Scientific

The University of New Mexico

# Superparamagnetic Particles and the Detection and Imaging of Disease

## Measuring the Remanence Fields

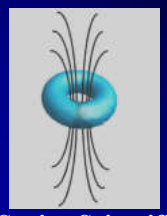

Senior Scientific

The University of New Mexico

# 7-Channel SQUID Measuring Chamber

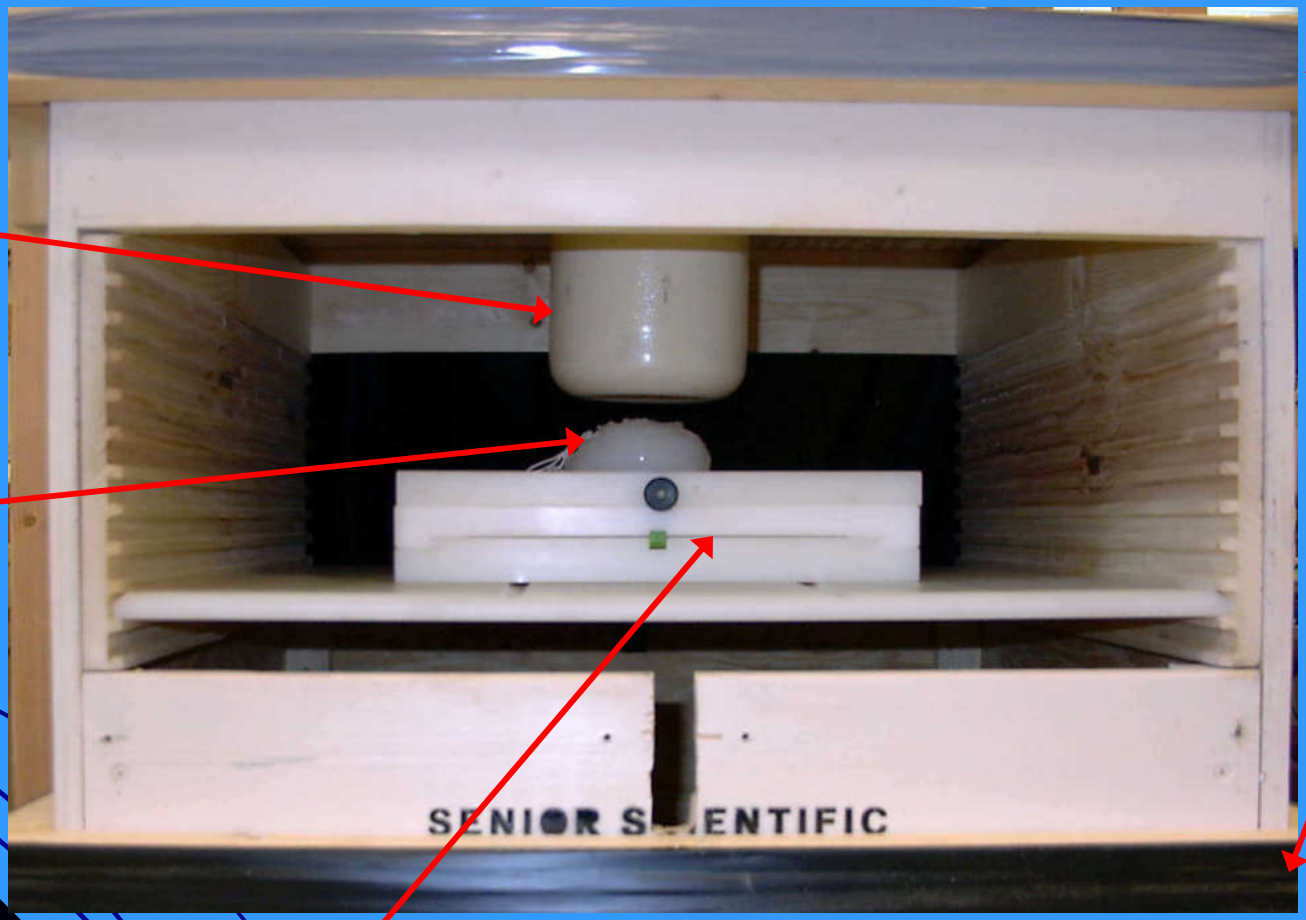


SQUIDs

Cell Source

Helmholtz Coils

Non-Magnetic Stage

Multi-channel system permits vector moment measurements

Senior Scientific

The University of New Mexico

# Second-order gradiometer Sensor Array

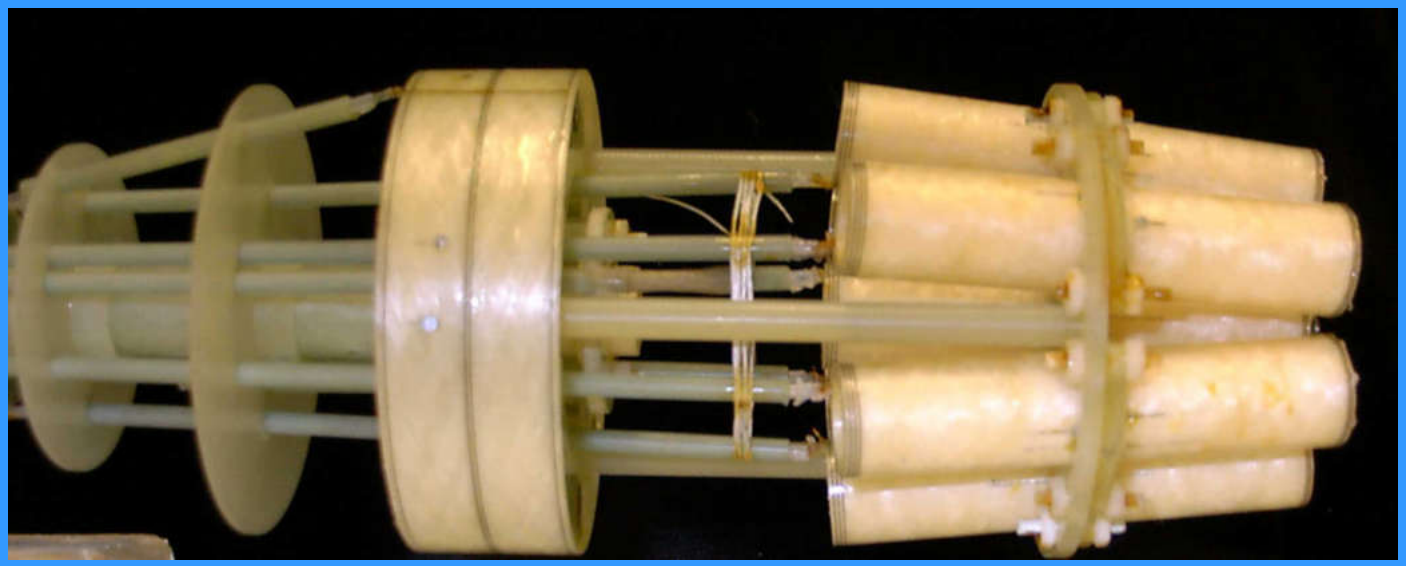

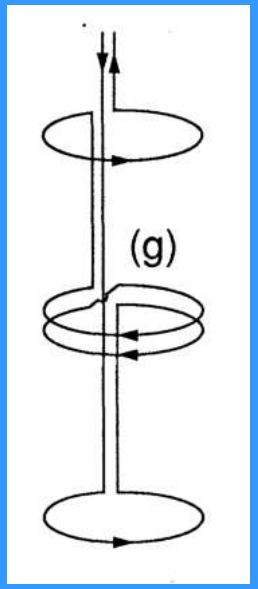


Measures 2nd derivative of magnetic field to minimize background pickup of external fields. Permits operation without the need for a magnetically shielded room.

Senior Scientific

The University of New Mexico

# Methodology

## Procedure for Measuring Remanence Fields

1) Antibody-nanoparticles injected into subject (< 1mg Fe).
2) Subject placed under sensor system
3) Magnetizing pulse applied (38 Gauss applied for 0.30 sec)
4) Remanence fields measured for two Seconds
5) Magnetic moment and location of source(s) obtained
6) Number of detected cells determined

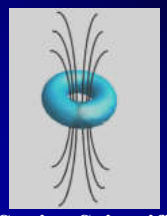

Senior Scientific

E R Flynn and H C Bryant, "A biomagnetic system for *in vivo* cancer imaging," Physics in Medicine and Biology **50** (2005) 1273-1293

The University of New Mexico

# Example of 7-channel SQUID remanence fields

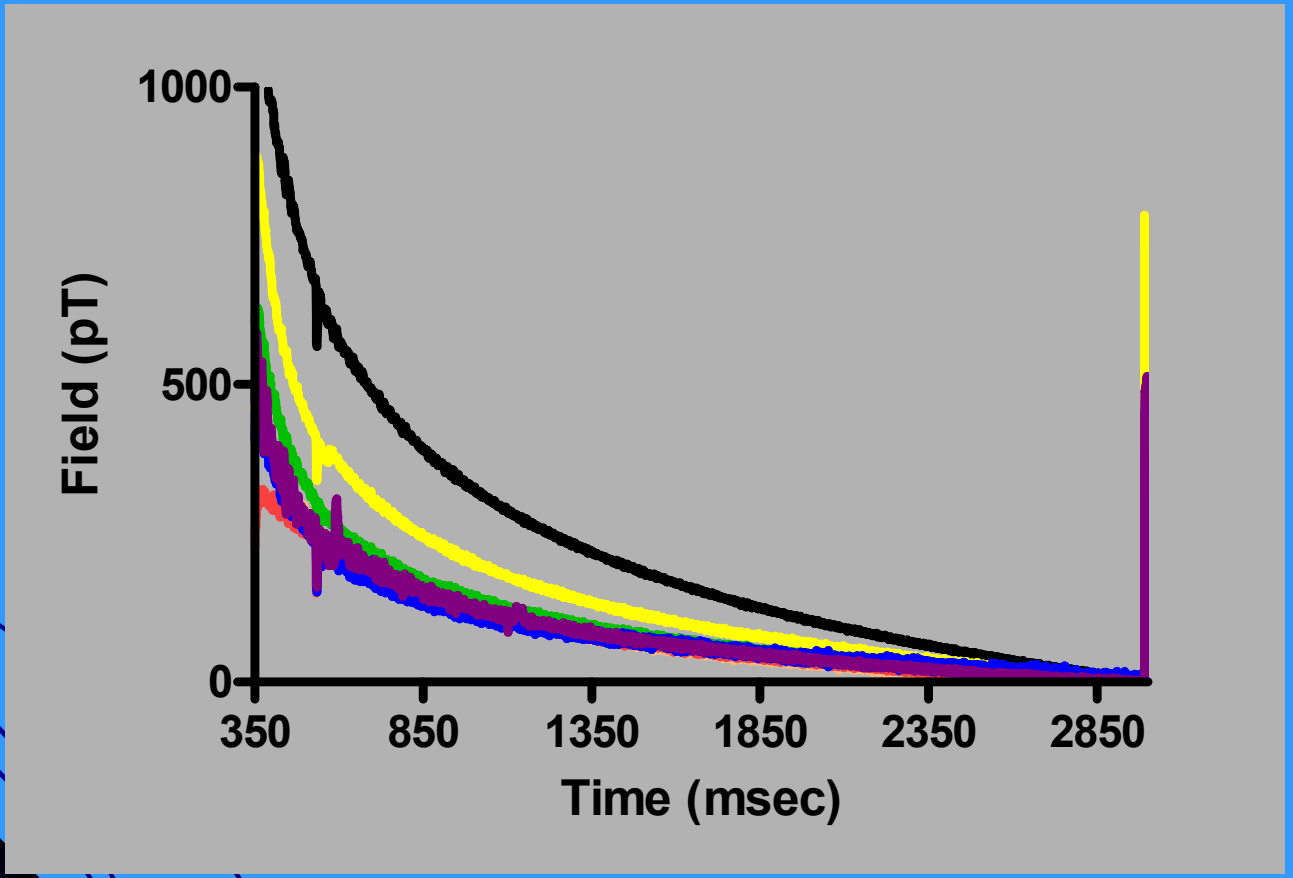


Senior Scientific

The University of New Mexico

# Disease detection procedure

## Calibrate Cell Sensitivity:

- Measure magnetic moment per particle by fitting magnetization curve to Langevin function
- Measure magnetic moment of cell sample with known number of cells
- Calculate number of nanoparticles/cell for each cell type

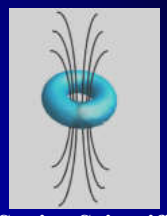

Senior Scientific

The University of New Mexico

# Superparamagnetic Particles and the Detection and Imaging of Disease

## Detecting and Locating Cancer

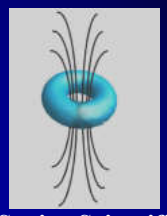

Senior Scientific

The University of New Mexico

# Clinical Arrangement in unshielded environment

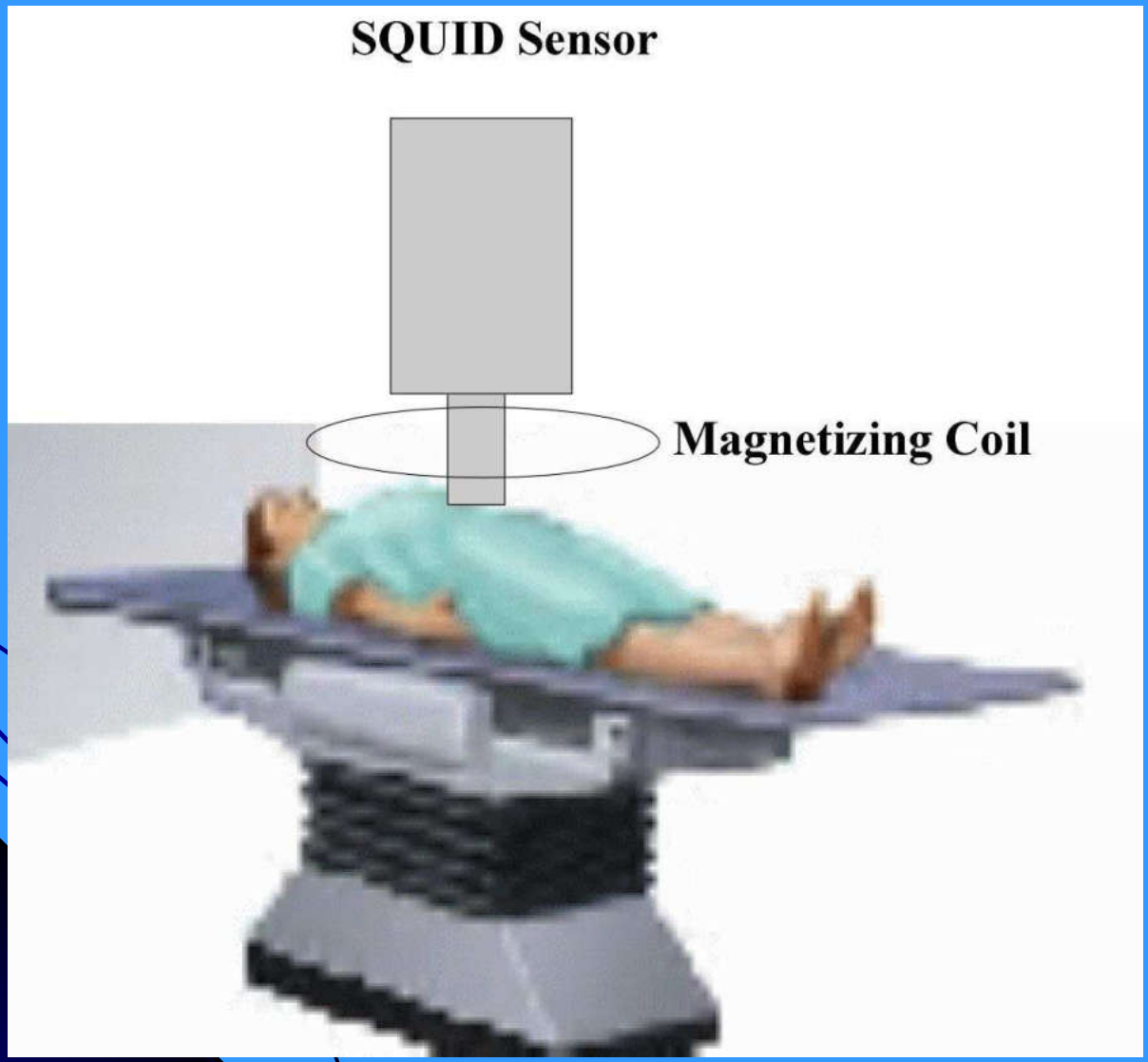


Senior Scientific

The University of New Mexico

# Growth of human tumor

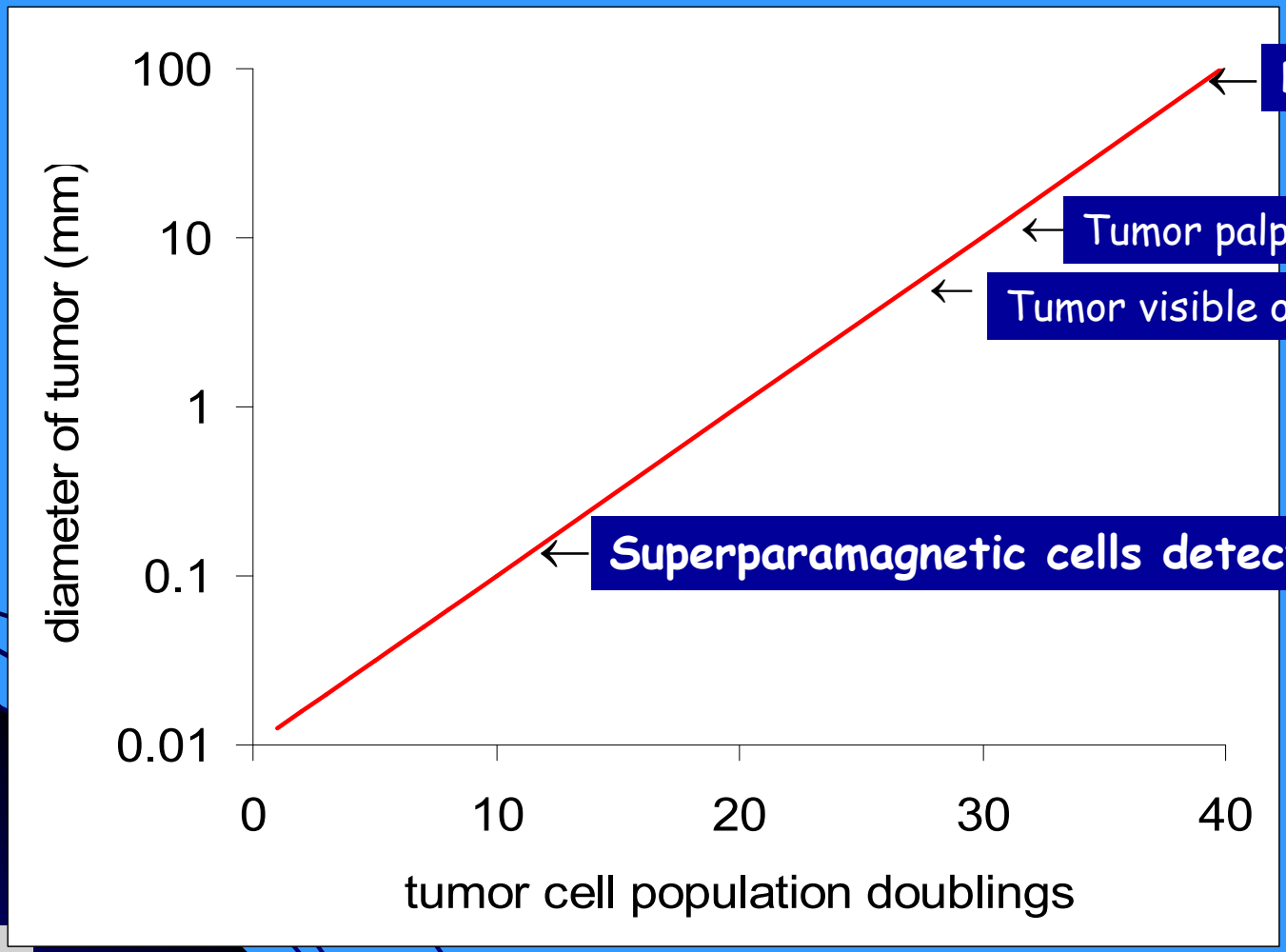


Reference: *The Cell* p. 1316

Senior Scientific

The University of New Mexico

# Breast Cancer

Breast Phantom with two vials of live breast Cancer cells (MCF-7) Coupled to Magnetic nanoparticles with HER-2 antibodies

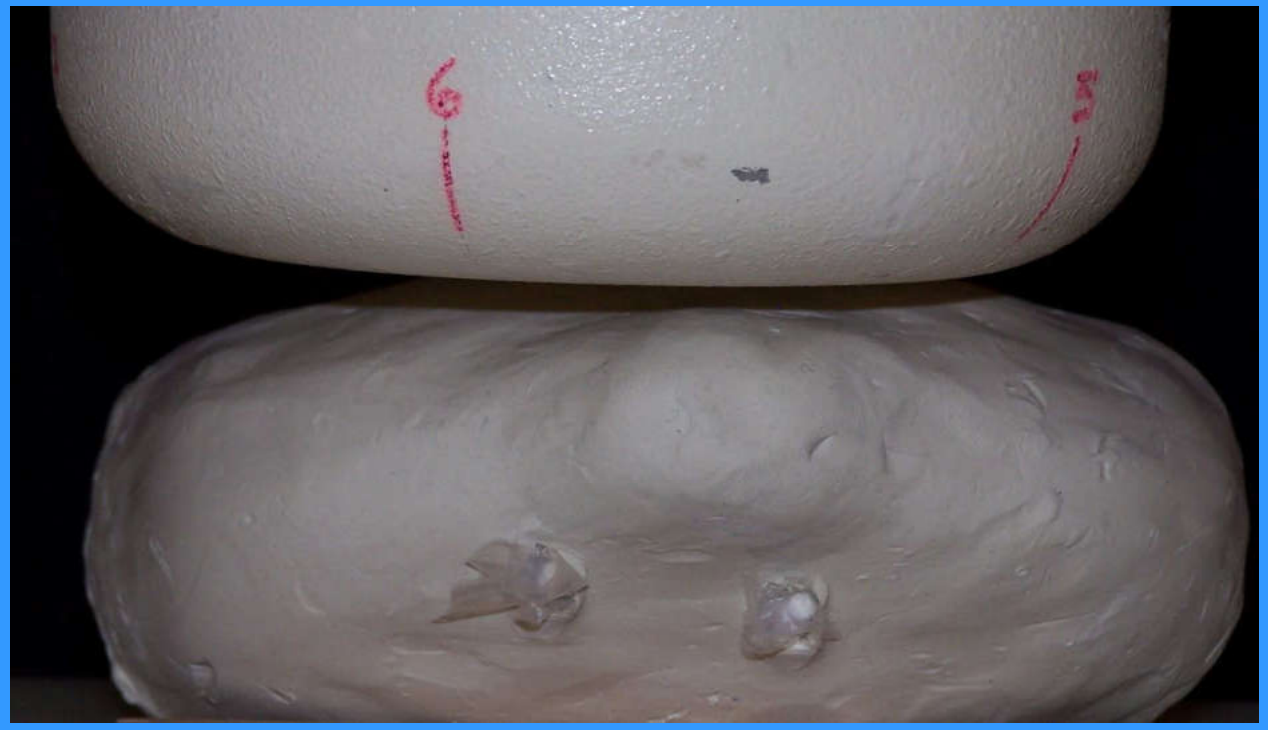

Sensitivity for breast cancer cells = $10^5$ cells for depths up to 8 cm into breast. Imaging accuracy is +/- 3 mm.

Senior Scientific

The University of New Mexico

# Breast Cancer Markers and Cell Lines currently under study

**Antibodies:**

HER-2 antibodies

CA27.29 Breast Tumor Marker present on epithelial cells and elevated in breast cancer (33% in early and 67% in late stage cancer)

CA15-3 also elevated but not as specific

**Angiogenesis:**

*VIP01 (vascular imaging peptide 01)* binds to the integrin $\alpha_v\beta_3$ shown to be overexpressed at sites of neovascularization and metastasis.

**Cell Lines Available:**

BT-549, MDA-MB-436, MDA-MB-134-VI, HCC202, HCC1008, ZR-75-1, T-47D, MDA-MB-231, and BT-474.

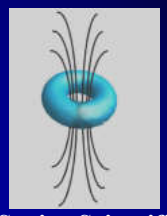

Senior Scientific

The University of New Mexico

# Mouse Model of Human breast cancer

SCID Mouse with human breast cancer Xenograft on flank.

MCF7 Cancer Cells

Mouse injected with Nanoparticles coupled to HER-2 antibodies

Senior Scientific

The University of New Mexico

# Results of Mouse Tumor Study

Magnetic moment (x 1E+07 A-m$^2$)

as a function of time from mouse tumor after injection of nanoparticles.

$\mu$ = 1.0 = 2.6x10$^{10}$ nanoparticles = ~ 3 x 10$^6$ cancer cells

(~1 x 10$^4$ np/cell)

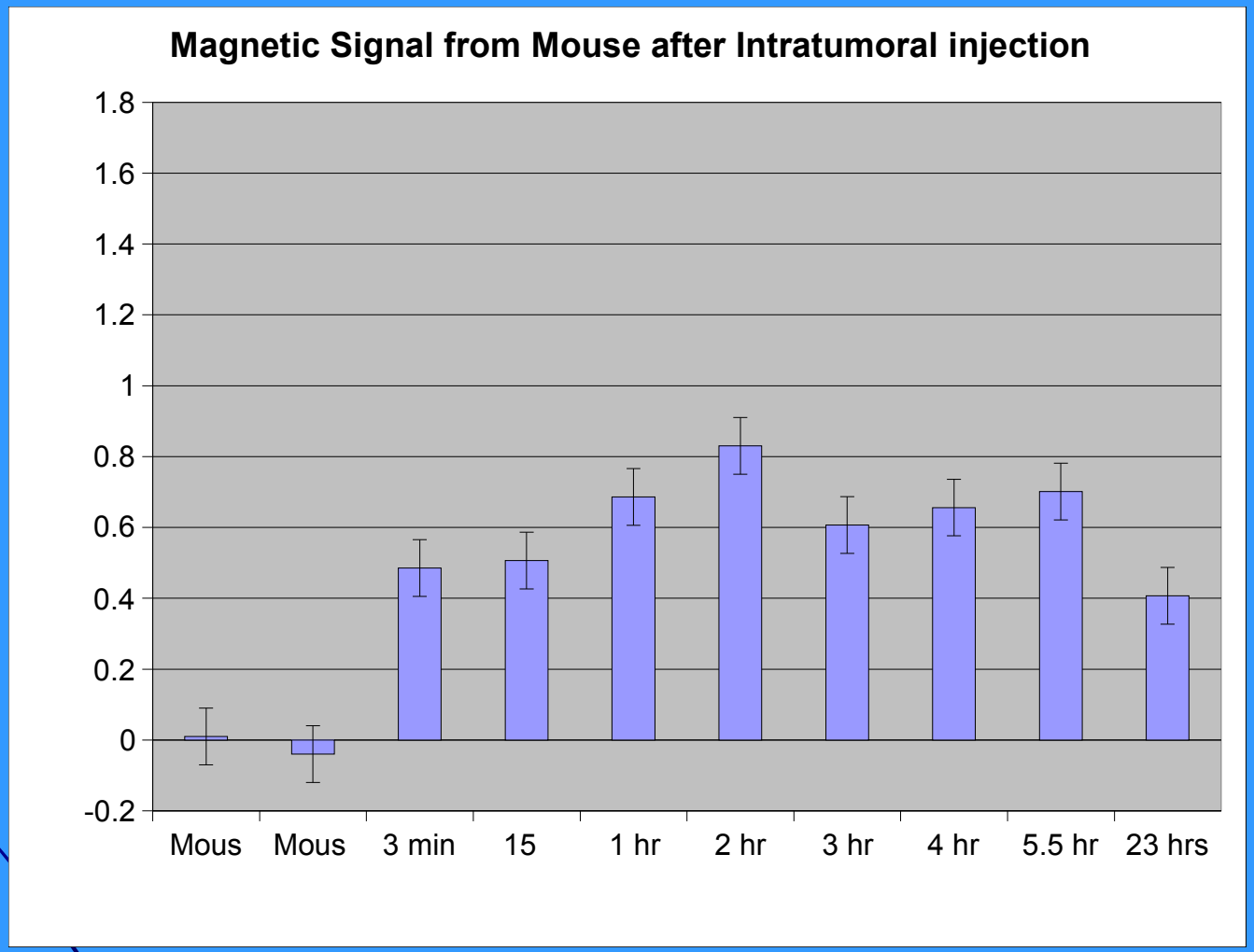


Senior Scientific

The University of New Mexico

# Labeling of Breast Cancer Cells with magnetic NP

BT474 breast tumor cells, labeled with SiMag 1411 Carboxyl magnetic NP, coupled to anti-her2 Ab. Left is bright-field image of BT474 cells showing NP bound to surface, Right image is dark-field image.

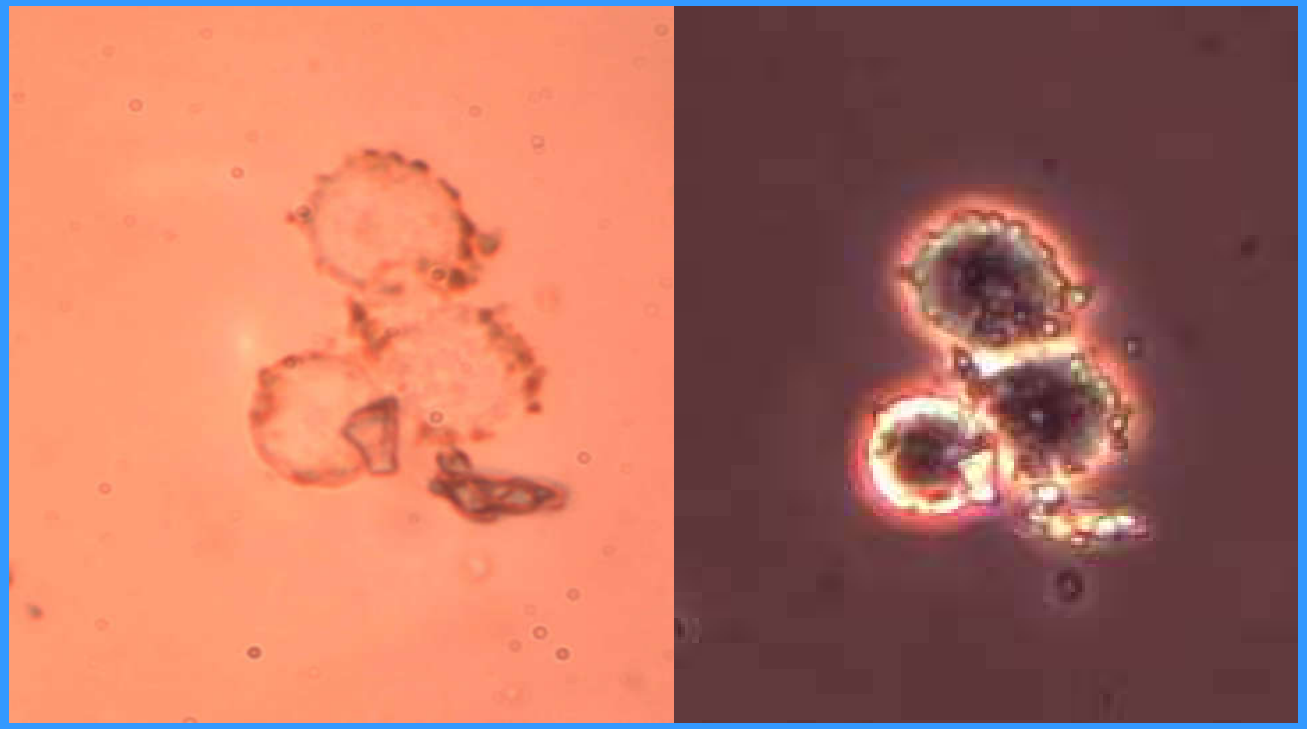

Senior Scientific

The University of New Mexico

# Ovarian Cancer

Anatomical Model under sensor system.

Ovary with Carcinomas

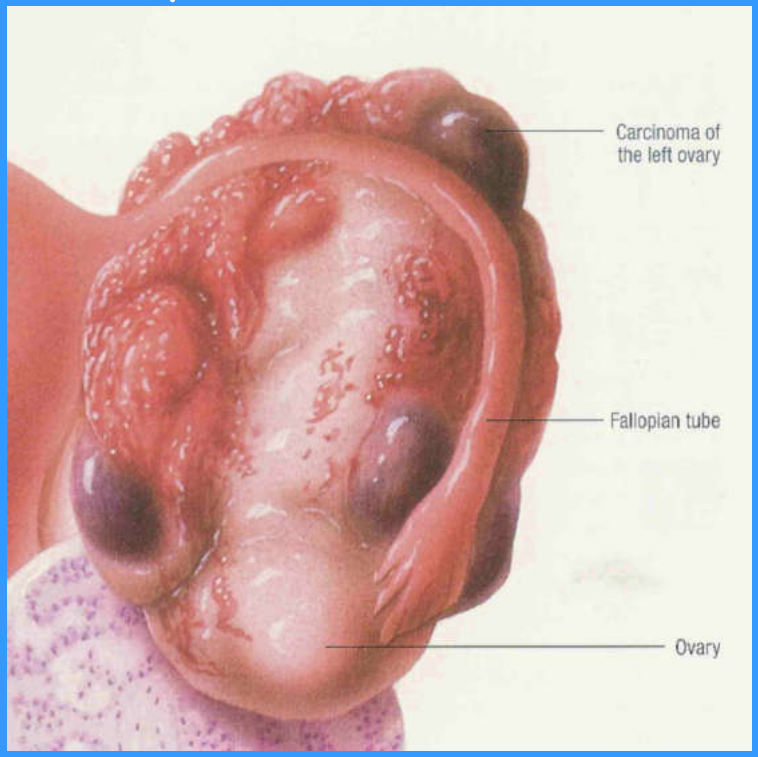


Nanoparticle in-vivo imaging permits several consecutive injections of different markers to improve sensitivity and specificity; e.g., CA125 & HMFG1/G2 give
95% sensitivity 93% specificity

Senior Scientific

The University of New Mexico

# 7-channel SQUID remanence fields from 500,00 live ovarian cells coupled to nanoparticles with CA-125 markers.

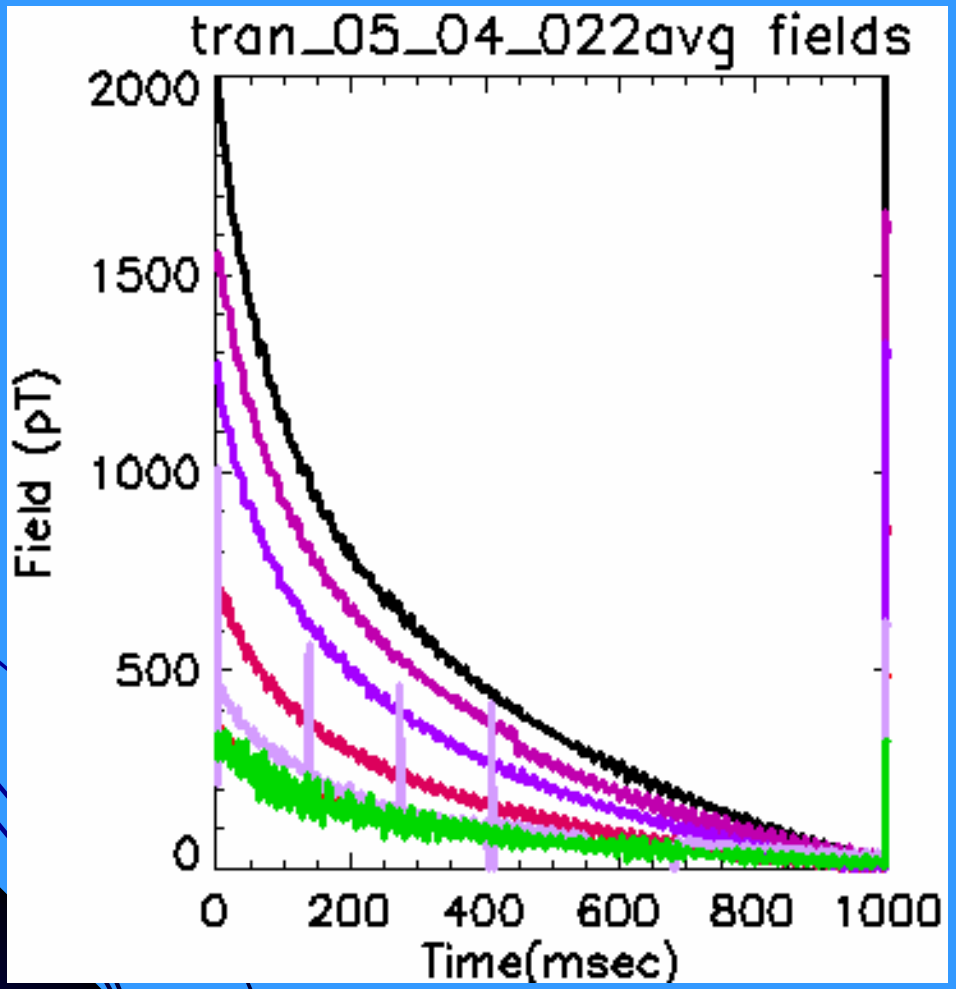


Senior Scientific

The University of New Mexico

# Live Ovarian Cell lines

**Marker: CA125**

| *Cell Line* | *NP/cell* |
|---|---|
| tov-112D | 2.04 x$10^4$ |
| ov-90 | 3.35 x $10^3$ |
| ovcar-3 | 6.73 x $10^3$ |

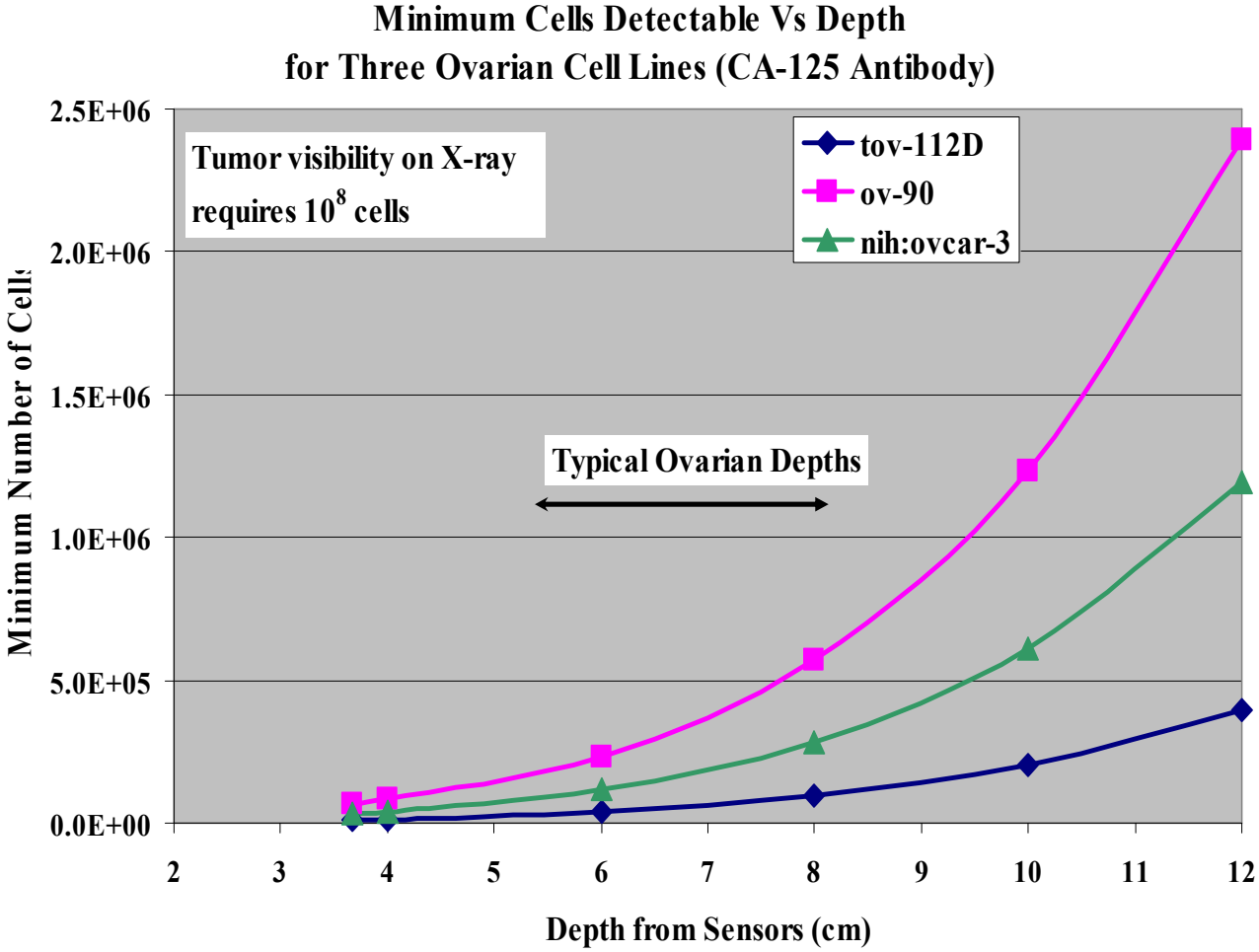


Senior Scientific

The University of New Mexico

# Superparamagnetic Particles and the Detection and Imaging of Disease

## Detecting Rejection of Transplanted Organ

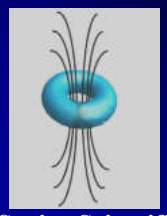

Senior Scientific

The University of New Mexico

# In-Vivo Detection of the Rejection of a Transplanted Organ

1) Rejection of a transplanted organ occurs by T-cells that attach to foreign Human-Leukocyte-Associated antigens on the donor cells and kill them.
2) T-cells accumulate in small nodules within the organ.
3) T-cells can be targeted with specific antibodies, conjugated to magnetic nanoparticles, and detected in-vivo by SQUID sensors.
4) Method minimizes the need for painful biopsies.
5) Monitoring for T-cell presence will be used to determine the amount of anti-immune system drugs being administered.

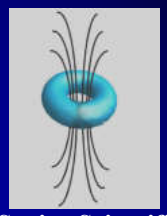

Senior Scientific

The University of New Mexico

# Each T-cell will have 5 x $10^4$ CD3 Antibodies conjugated to nanoparticles

1) Current SQUID system detects $10^5$ cells at 4 cm and $10^6$ at 8cm.
2) This corresponds to the amount in ~100 micron diameter nodules.
3) Completely rejected organ may contain $10^{10}$ - $10^{11}$ T-cells.
4) Transplanted organs include kidney, heart, liver and lung.

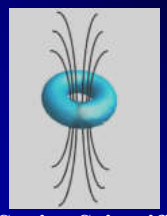

Senior Scientific

The University of New Mexico

# Specific Binding of Nanoparticles to Cells

Jurkat T-Cells CD2 Antibody (non-specific)

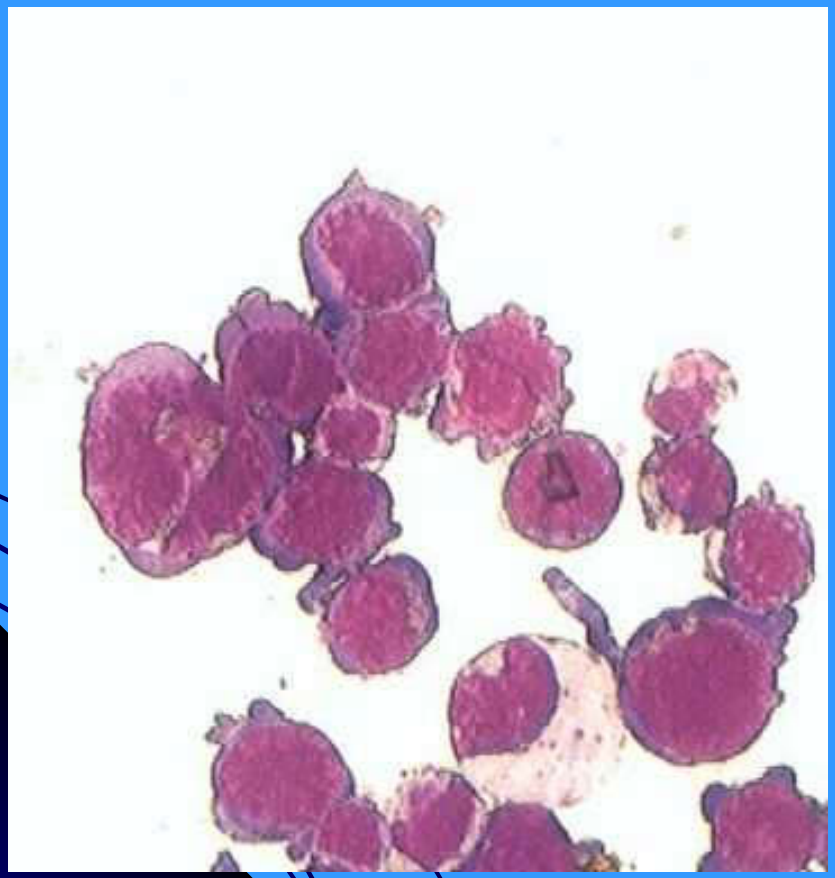

Jurkat T-Cells +CD3 Antibody (specific)

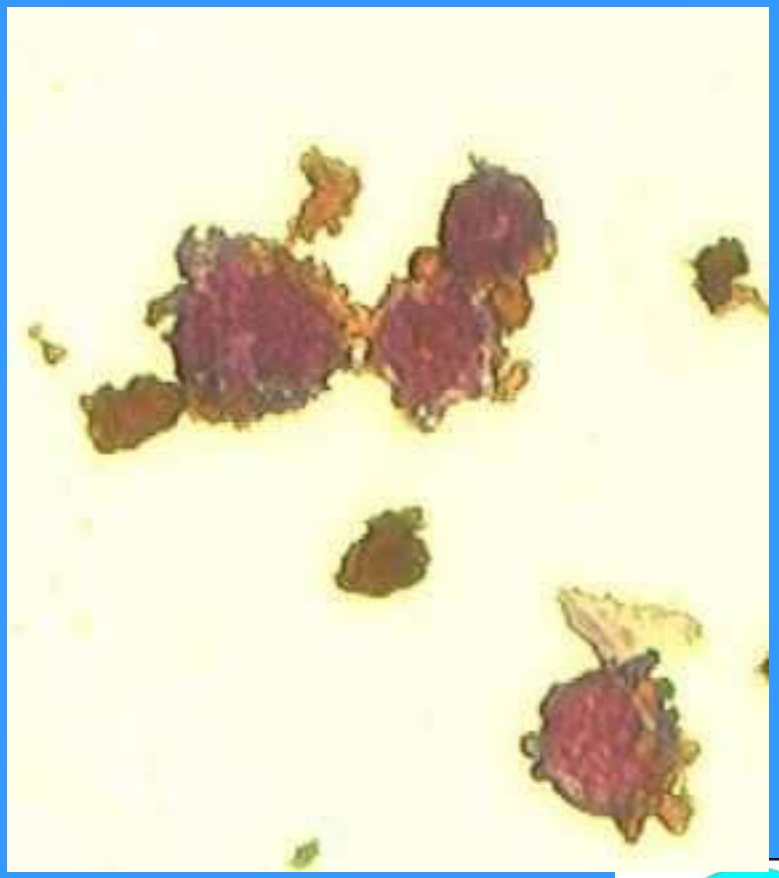

Jurkat cells are leukemia T-cells

Senior Scientific

The University of New Mexico

# Kidney Phantom containing two sources of Live Jurkat T-cells under SQUID sensor

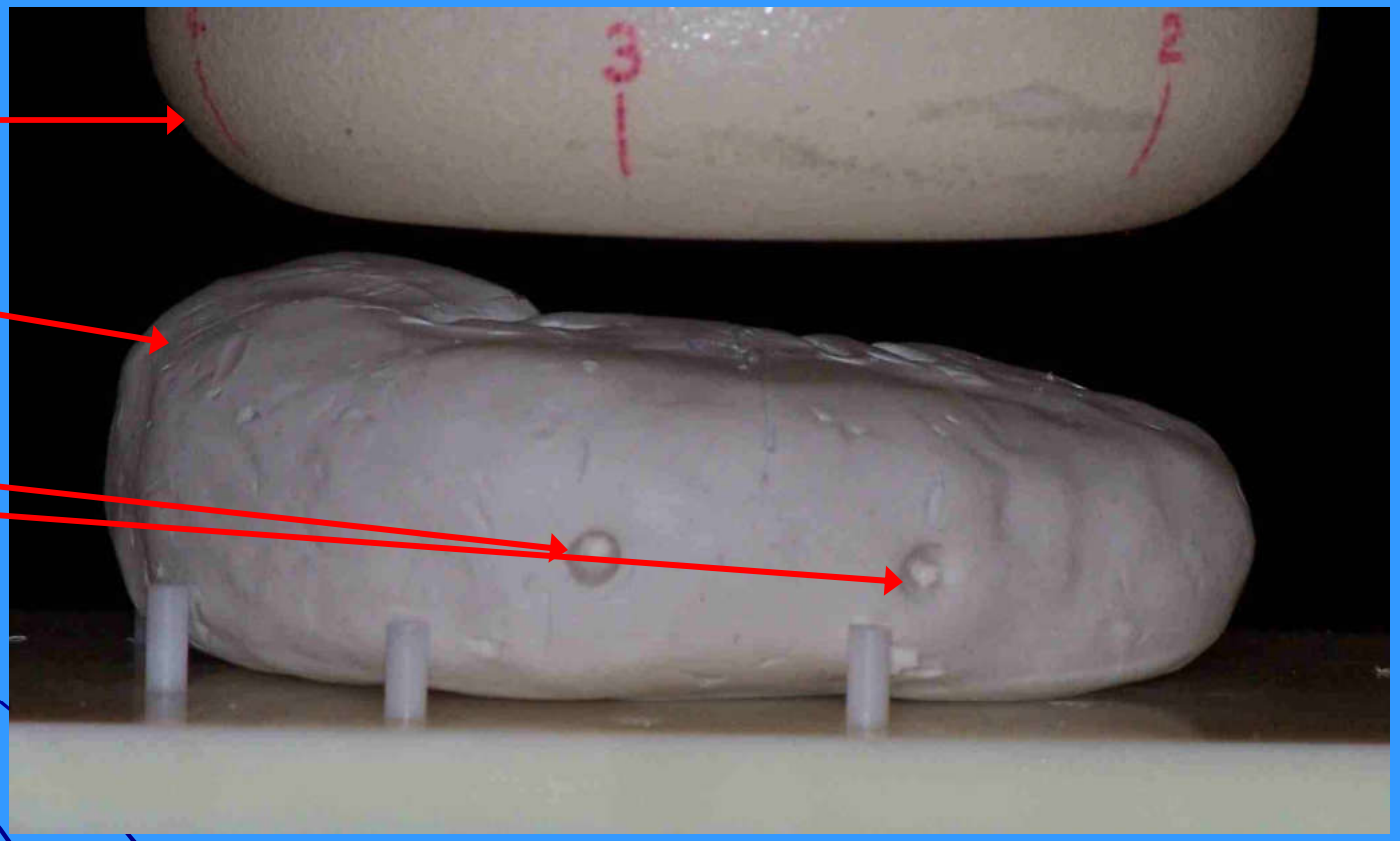

# Magnetic Field Contours of Data and Theory for two Live Cell Sources in Kidney Phantom

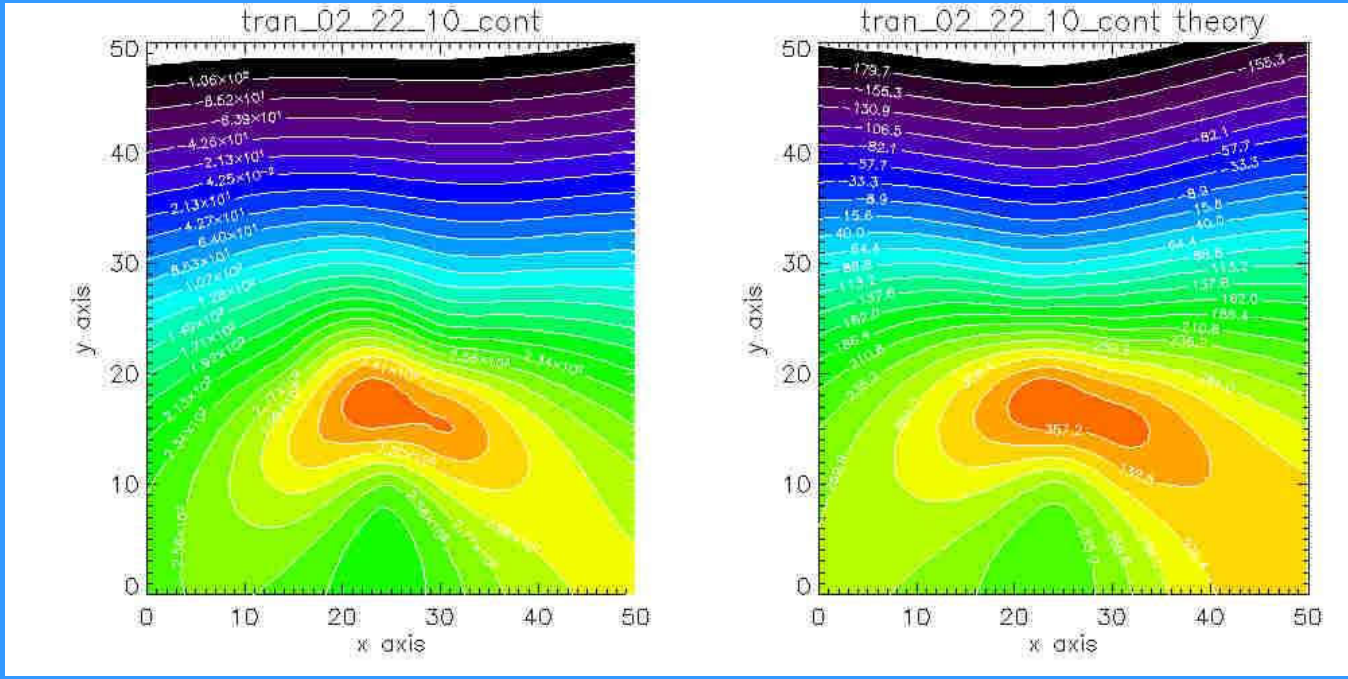


Data Contours

Theory Contours

| Source 1 | x | y | z | m(A-m$^2$) | Cells |
|---|---|---|---|---|---|
| measured | 1.4±.3 | -1.1±.3 | 5.5±.3 | 1.52E-07 | 4.3E+06 |
| imaged | 1.3±.4 | -1.9±.4 | 5.0±.3 | 1.45E-07 | 4.1E+06 |
| Source 2 | | | | | |
| measured | -2.7±.3 | -1.5±.3 | 5.5±.3 | 1.60E-07 | 4.6E+06 |
| imaged | -2.7±.4 | -2.2±.3 | 5.0±.3 | 1.60E-07 | 4.6E+06 |

Senior Scientific

The University of New Mexico

# Superparamagnetic Particles and the Detection and Imaging of Disease

## Diseases of the Brain

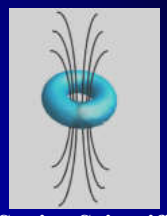

Senior Scientific

The University of New Mexico

# Diseases of the Brain

Nanoparticles and SQUID detection can be used to detect, and potentially treat, disease's of the brain; e.g., Alzheimer's and Multiple Sclerosis.

Specific coatings such as PEG help to get past the BBB with magnetic nanoparticles carrying Antibodies and Drugs

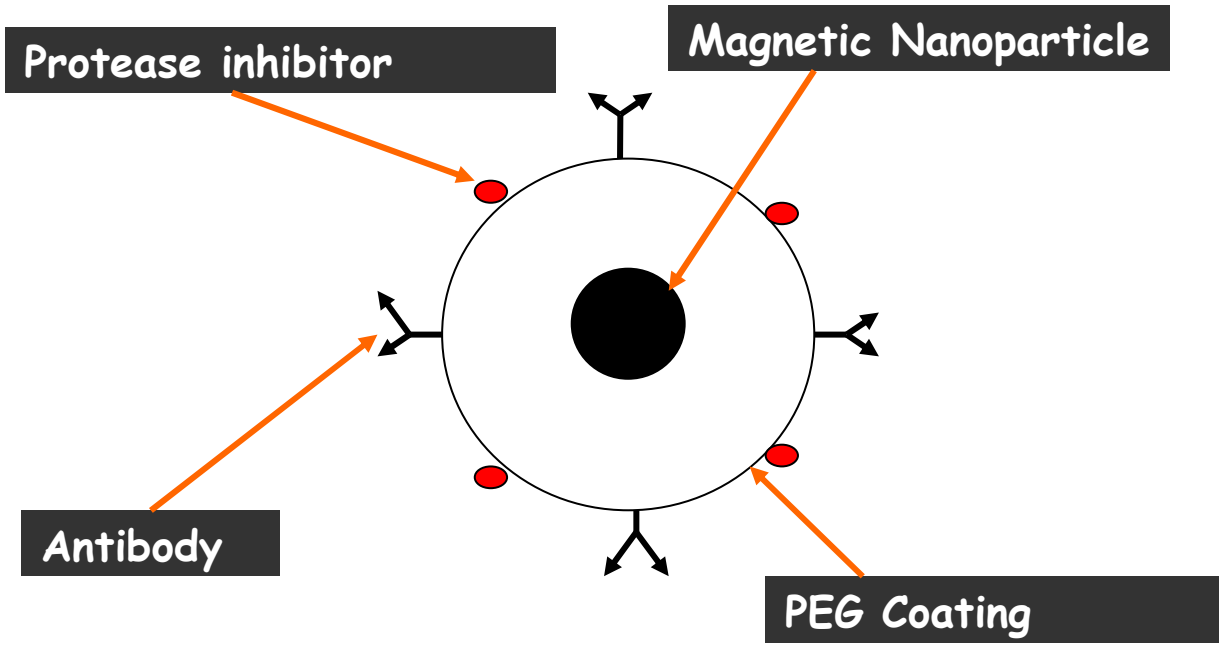


Senior Scientific

The University of New Mexico

# Methodology of Detection and Treatment of AD

1) Use nanoparticles coated with PEG to get by BBB
2) Use antibodies for Amyloid Plaque and Tau
3) Inject into patient and detect and localize plaque and Tau deposits
4) Determine presence and state of AD
5) Inject nanoparticles with antibodies and anti-plaque drug
6) Magnetically concentrate particles over localized plaque sites

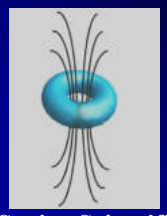

Senior Scientific

The University of New Mexico

# Measuring Sources in the Brain

Model of brain placed in skull with multiple diffuse nanoparticle sources to measure multiple extended sources

Senior Scientific

The University of New Mexico

# Localization of Nanoparticle Sources in the Brain

## Experimental Fields

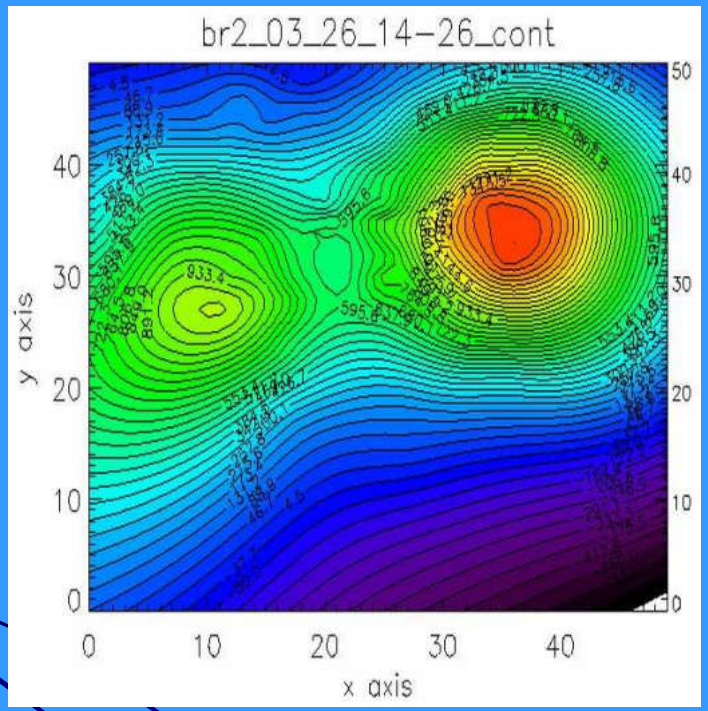


## Theoretical Fields

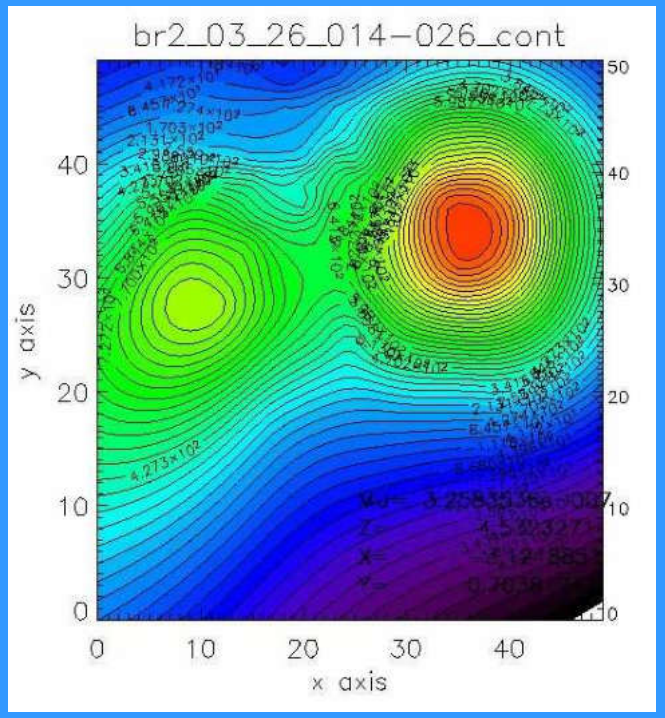


| Dipole1: | X | Y | Z | M | N |
|---|---|---|---|---|---|
| | -3.12 | 0.70 | 4.53 | 3.26 | |
| | 7.2E+10 | | | | |

| Dipole2: | X | Y | Z | M |
|---|---|---|---|---|
| | 2.19 | 1.85 | 4.31 | 4.07 |

Senior Scientific

The University of New Mexico

# Alzheimer Disease Status

1) Primary Imaging analysis completed

2) Antibodies for Amyloid Plaque and Tau

3) Antibodies coupled to Nanoparticles

4) Flash-frozen brain slices of AD Patients

5) AD Mouse model under development
(UMN have developed AD mouse)

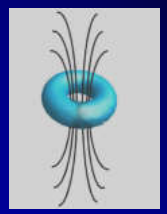

Senior Scientific

The University of New Mexico

# Summary

(1) SQUID sensor sensitivity can detect and image brain magnetic fields and targeted nanoparticles in disease.
(2)Measurement of natural biomagnetic fields can be used to understand brain function
(3)Measurement of natural biomagnetic fields can be used to understand the working mind
(4) Magnetic nanoparticles and weak field sensors can be used for early disease detection.
(5)Nanoparticle applications include cancer, leukemia, transplant rejection, and brain diseases.
(6) Treatment options include multi-function nanoparticles for localization and magnetic concentration or hyperthermia.

This research was funded in part by:

The National Cancer Institute

The National Institute for Allergies and Infectious Disease

The US Department of Defense

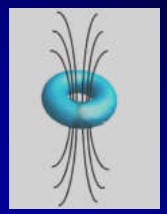

Senior Scientific

The University of New Mexico

# Primary Participants

E. R. Flynn[1],
H. C. Bryant[1,3],
D. A. Sergatskov[1,4],
R. S. Larson[3], D. Lovato[3], L. Sillerud[3], J. Jaetao[3]
N. Adolphi[2]
C. Bergemann[5]
D. Huber[6]
A. Georgopoulos[7], A. Leuthold[7]

[1]Senior Scientific,LLC, [2]New Mexico Resonance
[3]University of New Mexico, [4]FermiLab,
[5]Chemicell GmbH, Germany, [6]CINT-Sandia National Lab,
[7]VA Hospital and UMN, Minneapolis, MN

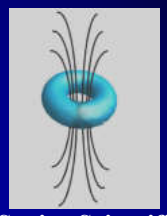

Senior Scientific

The University of New Mexico